

Viewer-Centered Frame of Reference for Pointing to Memorized Targets in Three-Dimensional Space

J. MCINTYRE, F. STRATTA, AND F. LACQUANITI
Istituto Scientifico S. Lucia, I.N.B.-C.N.R., 00179 Rome, Italy

McIntyre, J., F. Stratta, and F. Lacquaniti. Viewer-centered frame of reference for pointing to memorized targets in three-dimensional space. *J. Neurophysiol.* 78: 1601–1618, 1997. Pointing to a remembered visual target involves the transformation of binocular visual information into an appropriate motor output. Errors generated during pointing tasks may indicate the reference frames used by the CNS for the transformation and storage of the target position. Previous studies have proposed eye-, shoulder-, or hand-centered reference frames for various pointing tasks, depending on visual conditions. We asked subjects to perform pointing movements to remembered three-dimensional targets after a fixed memory delay. Pointing movements were executed under dim lighting conditions, allowing vision of the fingertip against a uniform black background. Subjects performed repeated movements to targets distributed uniformly within a small (radius 25 mm) workspace volume. In separate blocks of trials, subjects pointed to different workspace regions that varied in terms of distance and direction from the head and shoulder. Additional blocks were performed that differed in terms of starting position, effector hand, head rotation, and memory delay duration. Final pointing positions were quantified in terms of the constant and variable errors in three dimensions. The orientation of these errors was examined as a function of workspace location to identify the underlying reference frames. Subjects produced anisotropic patterns of variable error, with greater variability for endpoint distances from the body. The major axes of the variable-error tolerance ellipsoids pointed toward the eyes of the subject, independent of workspace region, effector hand (left or right), initial hand position, and head rotations. Constant errors were less consistent across subjects, but also tended to point toward the head and body. Both overshoots and undershoots of the target position were observed. Increasing the duration of the memory delay period increased the size but did not alter the orientation of the variable-error ellipsoids. Variability of the endpoint positions increased equally in all three Cartesian directions as the memory delay increased from 0.5 to 8.0 s. The anisotropy of variable errors indicates a viewer-centered reference frame for pointing to remembered visual targets with vision of the finger. The anisotropy of pointing variability stems from variability in egocentric binocular cues as opposed to reliance on allocentric visual references or to specific approximations in the sensorimotor transformation. Nevertheless, observed increases in variability with longer memory delays indicate that the short-term storage of the target position does not simply mirror the retinal and ocular sensory signals of the visually acquired target location. Thus spatial memory is carried out in an internal representation that is viewer-centered but that may be isotropic with respect to Cartesian space.

INTRODUCTION

In arm reaching, a target location must be matched by a hand position. How does the brain solve this correspondence problem? When a stationary target is presented visually, its direction is mapped topographically onto the retina, whereas

its distance relative to the viewer is defined by both monocular cues (accommodation, relative size, intensity, perspective, shading, etc.) and binocular cues (retinal disparity and ocular vergence signals). Hand position can also be monitored visually. In addition, proprioception and efference copy of motor commands define arm posture in the intrinsic reference frames of muscles, joints, and skin receptors. The hypothesis has been put forth that, in the process of translating sensory information about target and arm position into appropriate motor commands, endpoint position of reaching may be specified in either shoulder-centered (Flanders et al. 1992; Soechting and Flanders 1989a,b) or hand-centered (Flanders et al. 1992; Gordon et al. 1994) frames of reference.

Experimental approaches often rely on the study of the errors made by subjects who point to a previously visible, memorized target, thus avoiding movement corrections based on visual feedback of a continuously present target (Prablanc et al. 1979). In this approach, differences in precision between independent neural channels for spatial information may reveal the underlying frames of reference putatively used by the brain (Soechting and Flanders 1989a). There are two types of errors for repeated trials with the same target location: constant (systematic) errors, representing the deviation of the mean endpoint from the target, and variable errors, representing the dispersion (variance) of the endpoints around the mean (Poulton 1981).

Soechting and Flanders (1989a) assessed the systematic errors made by subjects pointing in the dark to remembered target locations in three-dimensional (3-D) space. They found large undershoots of the radial distance of the more distal targets, with only negligible errors in direction. They were able to account for such errors by hypothesizing a linear, approximate transformation of the shoulder-centered coordinates of the target into the angular coordinates of the arm (Soechting and Flanders 1989b). An origin close to the shoulder for the coordinate system of movement direction was found by extrapolating a straight line from the target location through the final finger position to the frontal plane of the body (Soechting et al. 1990). When subjects pointed to remembered targets in full light, they reported that they used vision of background objects to align the direction of the finger with the remembered direction of the target. Accordingly, the origin of the coordinate system for movement direction was found to be at eye level (Soechting et al. 1990). Nevertheless, undershoots of target distance in full light were comparable with those measured in darkness (Soechting and Flanders 1989a). On the whole, these authors concluded that movements performed in the presence

or absence of visual feedback involve the same serial processes, including an obligatory transformation from head-centered to shoulder-centered coordinates (Flanders et al. 1992; Soechting et al. 1990).

The spatial analysis of constant errors may not be sufficient to reveal the underlying reference frames unambiguously. This is because biases in the mean endpoint are idiosyncratic to individual subjects and may also depend on the specific experimental conditions (Collewin and Erkelens 1990). Both undershoot (Darling and Miller 1993; Soechting and Flanders 1989a) and overshoot (Berkinblit et al. 1995; Foley 1975; Foley and Held 1972) of distal targets have been reported in the literature.

The spatial analysis of variable errors may contribute additional insight on the issue of the reference frames for reaching. In particular, the lack of correlation between endpoint variance along a specific set of coordinate axes would argue in favor of that particular coordinate system as the one used to encode endpoint positions (Bookstein 1992; Gordon et al. 1992; Lacquaniti et al. 1990). Gordon et al. (1994) analyzed the statistical distribution of variable errors in 2-D reaching movements. In these experiments subjects slid a hand-held cursor on a horizontal digitizing table so as to match the memorized position of targets displayed on a vertical monitor. The target and the screen cursor were blanked during movement, and vision of the hand was prevented, although feedback about movement accuracy was given after each trial. Under such experimental conditions, the variance of endpoint positions along the line of hand movement tends to be uncorrelated with the variance along the orthogonal line, in accordance with a hand-centered frame of reference. Bock (1986) has also argued for a hand-centered frame of reference on the basis of an observed accumulation of errors as subjects point to a series of targets without intermediate visual feedback about hand position. This observation argues for a programming of movement in terms of the magnitude of the displacement from the initial to final hand position. Overshoot and undershoot have been observed for monoarticular movements (Bock and Eckmiller 1986) and for movements in the frontoparallel plane (Prablanc et al. 1979). Although the undershoots noted for frontoparallel movement might be explained by an underestimation of the shoulder-to-target distance, as proposed by Soechting et al., undershoots in rotary movement around a fixed body axis (Bock and Eckmiller 1986) cannot. Furthermore, the magnitude of spatial errors depends on both the retinal locus of the visually presented stimulus and the target position relative to the body, whereas movement kinematics depends primarily on the position of the target with respect to the body axis (Fisk and Goodale 1985). Observed pointing errors might therefore reflect an underestimation of movement extent coupled in a nonlinear fashion with a distortion in the mapping from retinal to spatial coordinates.

The present study was undertaken to reexamine some of these issues by including a number of tests that have not been combined in previous studies. From a methodological standpoint, different workspace regions were probed with the use of the same locally uniform distribution of targets in 3-D. Each target location was repeated many times, in random sequence, by the accurate repositioning of a robot arm. Both constant and variable errors were computed and

compared with the use of 3-D statistics. The experimental protocols included pointing movements from different starting positions of the hand and use of either the right or the left arm. We performed a separate series of experiments to assess the effect of head rotations on pointing accuracy. The rationale behind all these protocols was to discriminate between viewer-centered, shoulder-centered, and hand-centered reference frames for the specification of endpoint position in reaching to memorized targets (Lacquaniti 1997). As a separate issue, we examined the effect of increasing memory delays. This latter manipulation of the pointing task was designed to ascertain whether target position is memorized in the same reference frame used for target acquisition or endpoint control. In all experiments, pointing movements were performed under dim light conditions, allowing successive vision of the target and hand against an unstructured black background. These viewing conditions were designed to test the role of different egocentric signals in reconstructing target and hand position and to exclude allocentric visual cues from the background.

METHODS

Subjects sat on a 45-cm-high straight-back chair facing a table measuring 150 cm wide \times 54.5 cm deep at a height of 69 cm. To the opposite edge of the table was fixed an upright flat backboard measuring 130 cm wide \times 85 cm high. Subjects were seated at \sim 20 cm from the front edge of the table (75 cm from the backboard). A headrest helped the subject maintain a constant head position throughout the experiment (Fig. 1), although the head was free to turn.

Point targets, in the form of a red 5-mm-diam light-emitting diode (LED), were presented to the subject by a 5-degree-of-

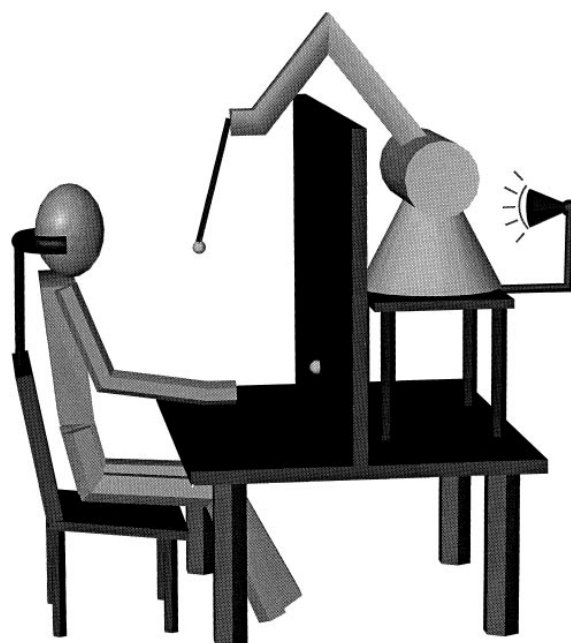


FIG. 1. Experimental conditions. Subject was seated in front of a black table and screen. Target, in the form of a red, 5-mm-diam light-emitting diode (LED), was presented by a robot in the space between the subject and a black screen. Small gray spheres: target LED attached to the robot arm and fixation LED located on the background screen. Low-level room lighting emanating from behind the screen resulted in a uniform black background behind the targets.

freedom robot (CRS Plus model A200). The base of the robot was situated behind the backboard and the LED was fixed to a 56-cm rod attached to the final link of the robot arm. The robot arm reached over the backboard and down to place the LED in the region between the subject and board (Fig. 1). The SD of repeated movements of the robot to the same target position was <0.25 mm in all three dimensions.

The board, the rod carrying the LED, and the top surface of the table were painted black. The room was dimly illuminated with indirect lighting coming from behind the backboard. Under these conditions, no discernible visual points could be seen directly behind the presented target. For a gaze orientation centered on the backboard, the visual field was uniform over a range of $\pm 40^\circ$ horizontally and $\pm 30^\circ$ vertically. Robot motion occurred only with the LED turned off and thus could not be seen. Except for the LEDs, room lighting was kept constant throughout a block of trials (15–20 min) to maintain a constant level of dark adaptation for the subjects.

Subjects performed a series of pointing movements in the following manner. The subject placed the index finger of the hand (left or right, depending on the experiment) on one of two starting positions located on the tabletop 10 cm from the front edge of the table and 20 cm to the right or left of the midline (depending on the experiment variant). The starting position was an upraised bump (2.5-mm-radius hemisphere) on the table surface that could be located by touch.

At the beginning of a trial, a green fixation LED located on the surface of the backboard at the midline, 13 cm above the tabletop, was illuminated. One second later an audible attention signal sounded. After a random delay of 1.2–2.4 s, the fixation light was extinguished and the red target LED of luminance 11.4 cd/m^2 (Gamma Scientific Digital Radiometer Model 2009 JR) subtending 0.5° at 60 cm was lighted at the target position for a period of 1.4 s, then extinguished and quickly removed. After a memory delay following the extinction of the target LED (0.5, 5.0, or 8.0 s, depending on the specific protocol described below), a second audible tone sounded, indicating that the subject should initiate the pointing movement. Subjects were instructed to place the tip of the index finger so as to touch the remembered location of the target LED. Subjects were instructed to attempt to maintain fixation of the remembered target position during the memory delay period. The subject had 2 s to perform the movement and hold at the remembered target position. Illumination of the finger was dim (0.0029 cd/m^2), but the finger was visible against the black background (0.0010 cd/m^2). Subjects could see the pointing finger throughout the movement while maintaining fixation at the target position. At the end of the 2-s period, a double or triple beep occurred, indicating that the subject should return the finger to the right or left starting position, respectively.

Positions and movements were measured by a four-camera Elite 3-D tracking system. At the beginning of the experiment, the coordinates of various body features were acquired by placing a reflective marker at each of the following points: centered on the top of the head, 2 cm above the midpoint between the eyes, at the right ear canal, at the shoulder, at the elbow, at the wrist, and at the fingertip. Measurements were taken with the right index finger positioned at the right hand starting position. For the measurement of the shoulder position, the marker was placed above the end of the scapula to approximate the location of the vertical axis of rotation for this joint.

During the experiment, the movement was measured by means of a reflective marker attached to the fingertip. The marker position was sampled at a rate of 100 Hz. A second marker attached to the forehead 2 cm above the midpoint between the eyes was also tracked during each trial. To measure the actual location of each target position, the subjects performed a set of 10 control trials in which they moved the index finger to touch the actual LED situated

at each of the target positions. This method of measuring the target position compensated automatically for the slight offset of the marker position with respect to the fingertip. Control trials were usually performed after all test trials, with some exceptions noted below.

The 3-D trajectory of the fingertip marker was computed for each trial. We calculated the initial and final position of each movement as the mean position computed over the first and last 10 samples, respectively, of the 2-s movement recording. A threshold based on the SD for these mean positions was used to reject trials in which the final endpoint position was not stable. Fewer than 2% of trials were rejected on this basis. The same SD of the final finger position within a single trial gives an estimate of the resolution of our measurements of the endpoint position. This estimate takes into account both the resolution of the Elite measurement system and the biological precision with which the subject holds a steady final position. For a typical experiment, the average SD was 0.16 mm.

We measured the variability of the finger position at the start of the movement across all trials. For a typical experiment, initial positions varied by <1 cm peak-to-peak, with an SD of 2.2 mm for X (left/right), 1.7 mm for Z (forward/back) in the horizontal plane, and 0.7 mm for Y (height), where the last axis was constrained by contact with the table.

Target configurations

Trials were performed in blocks of 90, with one block of trials lasting ~ 15 min. The number of blocks depended on the specific experimental design, as noted in the following text. Within a single block of trials, target locations were restricted to a relatively small volume in 3-D space. Different regions of the workspace were measured in separate blocks, depending on the experiment protocol. In the following, we refer to the location of the set of nine targets as the workspace region. The term “target position” refers to the exact position of a single target in space.

The primary constraint that led to the choice of target grouping was to provide a set of targets within a workspace region that had no readily discernible pattern or directional biases. A second goal was to present targets close enough together so as to encourage the subject to be as accurate as possible in determining the 3-D position in space. Subjects were told before beginning the experiment that the targets for a given block would appear within a small volume, but that the position of the targets would indeed vary in all three dimensions. It was further emphasized that the subject should place the fingertip at the exact position of the remembered target and not just point in the general direction of the remembered target location.

For a single workspace region, eight targets were distributed uniformly on the surface of a sphere of 22-mm radius, with a ninth target located at the center. This configuration is equivalent to points on the corners of a cube. The cube was tilted such that two opposite corners and the center formed a vertical line and was rotated to be symmetrical across the midline. The resulting distribution of points was left/right symmetrical across the vertical midline and up/down symmetrical across the horizontal midline when projected onto the frontal plane. The projection onto the horizontal plane produced a pattern that was both front/back and left/right symmetrical. The projection of the points into the sagittal plane did not produce an up/down or left/right symmetry; the top of the figure was “tilted” away from the subject (Fig. 2A).

Experiment protocols

Six variants of the basic experiment were performed, differing in terms of workspace location of the targets, choice of hand for pointing (left vs. right), starting position of the pointing hand, left-right rotation of the head, and memory delay duration. For all

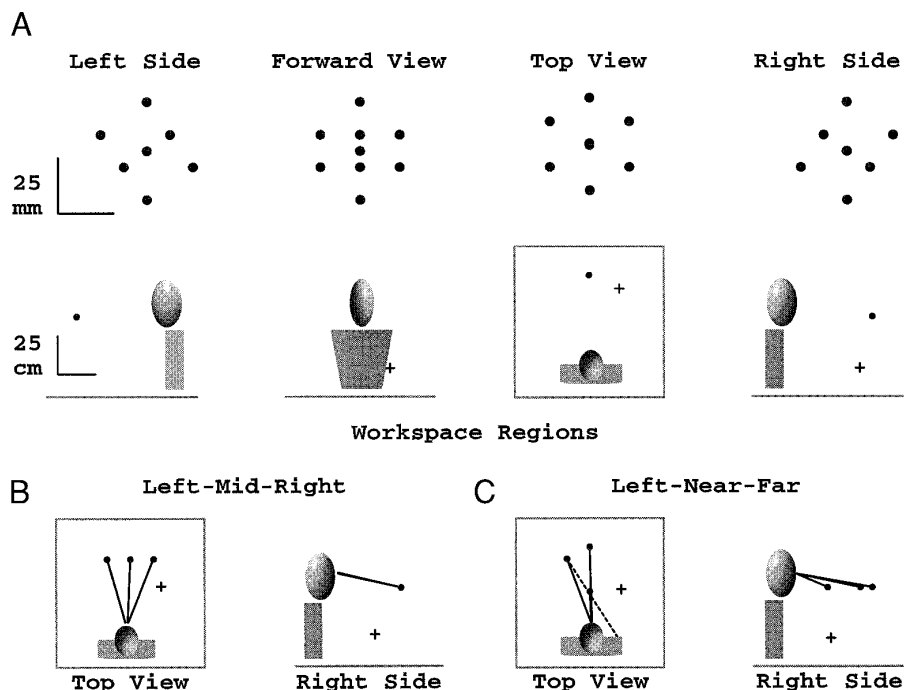


FIG. 2. Target positions for a single workspace region. Target positions were distributed evenly on a 22-mm-radius sphere. A: orthonormal projection views of the target positions from 4 different view-points (*top*) and the corresponding global view-point for each target view (*bottom*). In the global views, the size of the sphere represents the volume tested for a single workspace region. Plus signs: average finger position at the start of each pointing movement. B: workspace regions for the left-mid-right configuration. Nine targets were presented within each of the 3 separate regions. —, line-of-sight defined by the midpoint between the eyes and the center target position. C: workspace locations for the left-near-far configuration. Near and far workspace regions are aligned with the head; near and left regions fall on a line passing through the shoulder (---).

workspace locations, each target cluster was located ~ 10 cm above shoulder height (35 cm above the table) but varied in terms of distance from the subject and left or right displacement from the midline. For a given workspace region, subjects performed 20 trials to each of the nine target positions. Ten control trials were performed to each target position, either before or after the test trials, as noted below.

Only one workspace region was tested within a single block of trials. In all but one paradigm, the head was free to rotate. In general, subjects rotated the head to face the center of the target region being tested.

LEFT-MID-RIGHT. Six subjects performed pointing trials to three different regions of the workspace: the “left” location, located 14.5 cm to the left of the midline and 60 cm in front of the subject; the “middle” location, 60 cm in front of the subject along the midline; and the “right” location, 14.5 cm to the right of the midline and 60 cm in front of the subject (the mirror image of the left workspace location, see Fig. 2B). Subjects worked with the right hand and used only the right starting position.

Three of the subjects (AP, AR, and SC) performed the control trials after performing all test trials with a memory delay. Two subjects (SE and MS) performed all 10 control trials to each of the nine targets immediately before performing the test trials for a given workspace location. The last subject (FO) first performed, for each workspace location, several practice control trials to the center target only, then the test trials to remembered targets, and finally the complete set of control trials to all targets.

LEFT-NEAR-FAR. Four subjects performed the experiment with the right hand to targets in three different workspace regions, starting all trials from the right side. One set of trials was performed to the left target group, as in the left-mid-right paradigm above. A second workspace region was located along the midline, 68 cm in front of the subject (“far” targets). A third set of trials was performed to a group of targets located also on the midline, 38 cm from the subject (“near” targets). The left workspace location was chosen to lie on a line emanating from the right shoulder and passing through the center of the near target group (Fig. 2C). Furthermore, the distance from the right shoulder of the left target group was equal to that of the far target group. Thus we could

compare two pairs of target groups, the near and far targets, which fell on a line passing through the head, and the near and left targets, which lay on a line passing just above the right shoulder.

This configuration of target locations was designed specifically to test whether the origin of the coordinate system used for executing the task, as defined by the orientation of the variable-error distribution, is located at the head or the shoulder. If the origin is the head, one would observe a 30° counterclockwise rotation of the variable-error ellipsoid between the left and near targets, whereas the near and far major axes would be approximately parallel when projected onto the horizontal plane. Conversely, if the origin is at the shoulder, the near and left major axes would be roughly parallel, whereas the far axis would be rotated 14° clockwise with respect to the other two.

For the left-near-far configuration, all four subjects performed the control trials after having completed all trials to remembered targets. Note, however, that except for *subject FF*, all subjects had performed a similar experiment on a previous day to targets located in the far workspace region.

STARTING POSITION AND MEMORY DELAY. We tested the effects of starting hand position and memory delay duration in a single experiment. Six subjects performed pointing trials to the far workspace region. For this protocol, subjects performed trials with the 0.5-s memory delay used for all other protocols and additional trials with a memory delay of 8.0 s. Trials with the two different memory delays were randomly mixed within each block of 90. A pseudorandom sequence of trials was created, assuring that each target position was repeated five times for each memory delay. Subjects alternated the starting position for each trial (odd from left, even from right, or vice versa). By repeating the same pseudorandom sequence of target positions and memory delays, once starting the first trial from the left and once starting from the right, we were assured of having a total of five trials for each target position, each memory delay, and each starting position. Subjects performed four such pairs of blocks, resulting in 20 trials to each target position for each memory delay and each starting position (720 trials total). In a separate test of memory delay duration, two subjects performed the left-mid-right paradigm with a single, long (5.0-s) memory delay with the use of the right hand and the right starting position.

LEFT HAND. Three subjects performed the left-near-far protocol with the use of the left hand. Two of the subjects performed the experiment with the use of the starting position on the left side only. One subject (*JM*) performed trials alternating between the left and right starting positions, as described in the preceding text. Subjects performed the control trials after all test trials. It should be noted that all subjects had performed the experiment to the same set of targets on a previous day, including control trials, but with the use of the right hand.

HEAD ROTATION. Two subjects performed two separate sets of trials each, with the head rotated 26° to the left for one set or to the right for the other. Before each trial, the subject fixated an LED located 38 cm to the left or right of the midline, attached to the backboard 13 cm above the surface of the table. Subjects were required to maintain the eccentric head rotation throughout the trial, including the target fixation, memory delay, and movement execution. The head was lightly restrained with a cap and a string tied to a fixed post, blocking head rotation toward the central position. The far workspace location, as defined above, was tested for pointing with the right hand from the right-side starting position. Control trials were performed after all test trials. However, both subjects had performed the experiment on a previous day to the same set of targets with the head straight.

Subjects

A total of 13 right-handed subjects participated in the experiments, 4 males and 9 females aged 20–35 yr. The subject pool includes two of the authors (*JM* and *FS*). Informed consent was obtained from all other subjects, who were drawn from a school of physiotherapy. These subjects were informed of the overall nature of the experiment, but were unaware of the specific hypotheses being tested and the expected results.

Analysis of pointing errors

We computed both the constant errors made by the subjects (mean error to each target position) and the variable error (variance around the mean). The 3-D variable error was examined quantitatively in two ways. First we computed the eigenvectors of the variance and covariance matrix derived from the variability of responses to a given target. This provided an unconstrained estimate of the natural orientation of the coordinate system in which the target position is encoded without imposing a priori assumptions about the origin of that system. These measures were computed as follows.

Let t^i be the position of target i , and p_j^i be the final position of the finger for trial j to target i . The error Δ_j^i for a single trial is simply the vector difference between the final finger position and the target. The average final position for n^i repetitions to target i is denoted by \bar{p}^i . The constant error e^i for target i is given by the expression

$$e^i = \bar{p}^i - t^i \quad (1)$$

The deviation δ from the mean for a given trial is defined as

$$\delta_j^i = p_j^i - \bar{p}^i \quad (2)$$

The 3×3 matrix of variance and covariance (hereafter referred to as the covariance matrix) for a single target is given by the equation

$$S^i = \frac{\sum_{j=1}^{n^i} \delta_j^i (\delta_j^i)^T}{n^i - 1} \quad (3)$$

To obtain more robust statistical estimates, data may be combined to describe the average error within a single target group. The

overall average constant error e for all targets is simply the average constant error over all nine targets within a given workspace region. The underlying assumption for combining data in this manner is that the mapping of the intrinsic coordinate system of the subject to a standard Cartesian coordinate system is “smooth” and that targets within a single group were sufficiently close to one another such that errors produced at each target would be similar. The validity of these assumptions is discussed in the following text.

A single covariance matrix can also be computed for each workspace region, again to increase the statistical robustness. The combined covariance matrix is computed from the formula

$$S = \frac{\sum_{i=1}^k \sum_{j=1}^{n^i} \delta_j^i (\delta_j^i)^T}{\sum_{i=1}^k n^i - k} \quad (4)$$

Note that the deviation δ for a trial to a given target is computed relative to the mean of trials to only that target, not to the overall mean for all targets. The number of target positions k is subtracted from the total number of trials in the denominator to give an unbiased estimator of S based on k sample groups drawn from a population, with each group having its own mean (Morrison 1990, p. 100). The implicit assumption that pointing errors follow the same distribution for all nine targets is discussed in the following text.

The matrix S is the 3-D covariance about the mean for pointing to a remembered target. S can be scaled to compute the matrix describing the 95% tolerance ellipsoid on the basis of the total number of trials n

$$T_{0.95} = \sqrt{\frac{q(n+1)(n-k)}{n(n-k-q+1)}} F_{0.05, q, n-k-q+1} S \quad (5)$$

where $q = 3$ is the dimensionality of the Cartesian vector space (Diem 1963).

$T_{0.95}$ represents an ellipsoidal region around the mean response within which would fall 95% of all trials to a given target. The shape, size, and orientation of these ellipsoids were characterized by computing the eigenvalues and eigenvectors of the matrix $T_{0.95}$ with the use of the Jacobi method (Press et al. 1988). The size of the distribution is given by the eigenvalues $T_{0.95}$, the shape by the difference or ratio of the eigenvalues, and the orientation in space by the orientation of the three eigenvectors.

Because the estimates of the covariance matrices are based on a finite number of samples, the three computed eigenvalues will always differ, even for a population covariance that is truly isotropic. We can test whether any two eigenvalues are statistically distinct with the use of a χ^2 test of the form (Morrison 1990, p. 336)

$$\chi^2 = -(n-1) \sum_j \ln l_j + (n-1)r \ln \frac{\sum_j l_j}{r} \quad (6)$$

where l_j are the $r = 2$ eigenvalues being compared for a given covariance matrix ($j = 1-2$ or $j = 2-3$). This χ^2 statistic has $q = 1/2r(r+1) - 1$ degrees of freedom. Unless otherwise stated, we report and/or plot eigenvalues and their corresponding eigenvectors only if the given eigenvalue is significantly different from the other two at the 95% confidence level ($\chi^2 > \chi_{0.05, 2}^2$).

The eigenvector ω_i of a sample covariance matrix S is distributed as a multidimensional vector around the computed estimate. The tip of each eigenvector follows the multinormal distribution computed directly from the sample covariance matrix

$$V_i = \lambda_i \sum_{h=1}^p \frac{\lambda_h}{(\lambda_h - \lambda_i)^2} \omega_h \omega_h^T \quad (7)$$

Because the eigenvectors are constrained to have unit length, the distribution of tip locations is intrinsically described by a 2-D ellipse. However, because the ellipse may be oriented arbitrarily in 3-D space (in the plane perpendicular to the corresponding eigenvector), the ellipse is represented by the singular 3×3 matrix V of rank 2.

The accuracy of the estimate for the constant-error vector e is described by the 95% confidence ellipsoid $C_{0.95}$, which may also be computed from the sample covariance matrix

$$C_{0.95} = \sqrt{\frac{q(n-k)}{n(n-k-q+1)} F_{0.05, q, n-k-q+1}} S \quad (8)$$

where $q = 3$ is the dimensionality of the Cartesian vector space. To depict the accuracy of the direction of the constant-error estimate, the 95% confidence cones may be swept out for each estimated eigenvector by drawing rays from the true target position to points on the ellipsoid described by $C_{0.95}$. In a similar way, the accuracy of the variable-error eigenvector estimates can be shown by drawing the cone defined by the confidence ellipse for each eigenvector. The 95% confidence ellipse $V_{0.95}$ can be computed from V with the use of Eq. 8, with $q = 2$.

The results of one such set of calculations can be visualized in Fig. 3 from three different viewpoints as indicated in *column 1*. *Column 2* shows the cloud of 180 final finger positions combined from nine targets in a single workspace region. The line from the sphere representing the center target position to the center of the distribution depicts the average constant error e for the given workspace region. *Column 3* depicts the ellipsoid that contains 95% of the distributed points as computed from $T_{0.95}$. *Column 4* shows the major eigenvector of the covariance matrix emanating from the center of the distribution of points and scaled by 2 times the appropriate eigenvalue of $T_{0.95}$. The eigenvector is drawn surrounded by the confidence cone computed from $V_{0.95}$.

TESTS OF ASSUMPTIONS. Targets within a given workspace region were placed relatively close together (22 mm) so as to encourage the subject to work very precisely. This assumes that the subject can in fact distinguish differences between the nine target positions in all three dimensions. We tested this assumption by computing the correlation between the target position and the average final position for that target in each of the three Cartesian directions. Correlations were very significant ($P < 0.0001$) for all three axes, for all subjects, and for all workspace regions. Subjects were clearly able to discriminate between different target positions in all three dimensions.

The combining of data across trials to compute the average

constant error assumes that the constant error is similar for all nine targets within a single workspace region. This was not strictly the case. By an multivariate analysis of variance (MANOVA) test with target identification as a within-subjects factor, we can see a significant effect of the target factor on the 3-D error vector. Visual inspection shows that the average final positions for the targets on the surface of the sphere were biased toward the center of the sphere. However, because of the symmetrical distribution of targets on the sphere, biases for individual targets tend to cancel each other in the computation of the combined constant error. Constant-error vectors computed for the center target alone do not deviate substantially from the average error vectors computed across all targets.

By computing the covariance matrix based on data from all nine targets, one implicitly assumes that the distribution of errors is the same, or nearly the same, for all targets. We tested this assumption by comparing the covariance matrix computed for the 20 trials to the center target only with the covariance matrix S of Eq. 4. Estimates of the covariance orientation based on trials to the center target only were obviously noisier (larger confidence cones) but did not deviate systematically from the combined estimate. The major eigenvectors computed on the basis of combined data fell within the 95% confidence cones for the corresponding estimates based only on the center target. Thus we do not reject the null hypothesis that the two estimates are measures of the same statistical distribution, and we thus report results based only on the combined data, because of the greater confidence for these measures.

RESULTS

The purpose of these experiments was to search for a preferred reference frame as indicated by the pattern of errors observed for a manual pointing task. We looked for consistent changes in the constant and variable errors, defined in the preceding text, as a function of workspace location, starting position, choice of effector hand, and head orientation.

Workspace location

The most consistent indication of an inherent reference frame for pointing errors is given by the measurements of the variable error. In Fig. 4 we show the 95% tolerance ellipsoids for the experiments performed in the left-mid-right configuration. The ellipsoids are centered on the average final finger position for each of the three workspace regions.

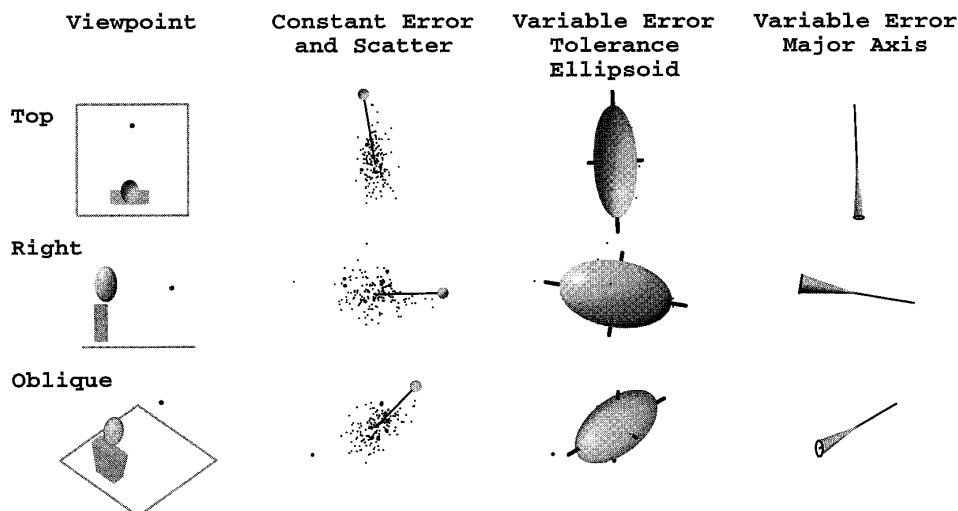


FIG. 3. Quantitative measures of errors in pointing by a single subject. *Column 1*: viewing orientation for each row. Small black sphere: range of target positions for the "mid" workspace region. *Column 2*: scatter of endpoint positions for a single workspace location. Data represent the combination of 20 trials to each of 9 real targets as described in METHODS. Small sphere: "virtual" target position at the center of all real target positions. Line segment: average constant error for all trials to the same workspace region. Cloud of points: variability of responses to a single target location, computed by combining data from all 9 targets. *Column 3*: tolerance ellipsoid that encompasses 95% of all data points within the distribution. *Column 4*: major axis of the 95% tolerance ellipsoid describing the variable error, surrounded by the 95% confidence cone for that axis.

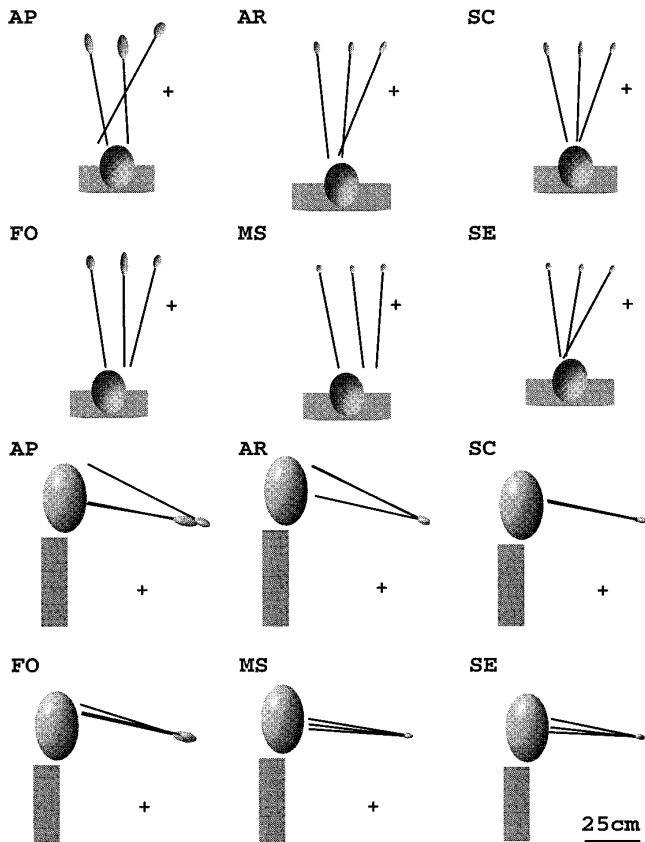


FIG. 4. Variable error for 6 subjects who performed the experiment to the left, middle, and right workspace regions. Ellipsoids represent the 95% tolerance region for a single target, computed from 20 movements to each of 9 targets. Lines emanating from each ellipsoid indicate the direction of the primary axis (1st eigenvector) projected to intersect with the frontal plane passing through the eyes. Plus signs: average starting hand position for all movements.

These ellipsoids are drawn to scale and are in general small with respect to the total workspace. The magnitude of the variable error is measured by the square root of the eigenvalues of the tolerance ellipsoid $T_{0.95}$, which are given in Table 1 for each subject and each workspace location.

The major eigenvector for each covariance matrix is plotted along with the ellipsoid in Fig. 4. The eigenvectors are extended in space toward the frontal plane that passes through the eyes of the subject. When viewed from either above or from the side, these vectors show a clear tendency to converge toward the head of the subject.

Figure 5 shows the same eigenvectors surrounded by the corresponding 95% confidence cone for each estimate. It can be seen that in almost all cases the head, and even more precisely the eyes, falls within the edges of the confidence cone, whereas in no case does the shoulder lie within the confidence region.

The variable errors for the left-near-far paradigm, shown in Fig. 6, give even stronger evidence for a head-centered reference frame. In three of four cases (*subject FS* is the exception) the major axis of the variable-error ellipsoid rotates significantly for the left workspace region, as compared with the near location, whereas the eigenvectors for the near and far locations are essentially parallel.

To test the statistical significance of these results, we first

performed an ANOVA on the direction (azimuth) of the covariance major eigenvector, with workspace region as a within-subject factor. For the left-near-far paradigm, we see a statistically significant effect of workspace location on the orientation of the major eigenvector [$F(2,6) = 8.16, P < 0.019$]. According to Scheffe's t -test for post hoc analysis, the azimuth of the major eigenvector differs significantly between the left and near workspace regions ($P < 0.036$) but not between the far and near regions ($P > 0.99$).

We tested two potential spherical coordinate systems, one with the origin at the eyes and a second with the origin at the right shoulder. Combining trials from all five workspace regions, there is no statistically significant difference between the direction of the major eigenvector of the covariance matrix and the direction of a line drawn to each workspace location from the head/eyes [$R(2,28) = 0.51, P > 0.60$]. The difference between the azimuth and elevation of such a line drawn from the shoulder to the workspace region is highly significant [$R(2,28) = 128.73, P < 0.00001$]. These results hold even if we consider only the left workspace region [$R(2,8) = 1.33, P > 0.31$ for the eye/head origin; $R(2,8) = 128.56, P < 0.00001$ for the shoulder origin].

No clear pattern emerges for the second and third eigenvectors. Whereas the first eigenvalue is distinct to a very high degree of confidence for all subjects and all conditions, the second and third eigenvalues are statistically different in only 50% of the cases (Table 1).

Measurements of constant error for the different workspace regions do not show the same consistency across subjects that was seen for measurements of variable error. For the left-mid-right protocol, the magnitude of the constant-error vector, shown in Table 2, varied from very small errors (*subject SC*) to rather large errors (*subject AP*). In Fig. 7 one can see both overshoots (*subjects AP* and *FO*) and undershoots (*subjects MS* and *SE*) of the true target position, where an overshoot is defined as a final finger position that is farther from the body than the real target position. Note that constant errors have been magnified by a factor of 5 to be discernible in the figure. Constant-error directions vary widely across subjects, although the direction of the vector is not very reliable when the magnitude is small (*subjects AR* and *SC*). When one considers only the larger constant-error vectors (*subjects AP, MS, and SE*), these vectors are roughly aligned with the head-target axis. All four subjects in the left-near-far experiment show a significant undershoot of the left and far targets (Table 2) and a tendency for these constant-error vectors to point toward the head (Fig. 8).

We computed a linear regression of target versus endpoint position for each of the three Cartesian directions independently for the six subjects who performed pointing to the mid-workspace region (Table 3). Slopes are significantly different from zero in all cases, confirming that subjects differentiated between targets in all three dimensions. Slopes for the Z dimension (depth) may be less than unity, indicating a compression of the average endpoint positions toward the center. Compression was greater in the Z (depth) dimension than for X (left/right) or Y (up/down) dimensions.

Starting position

Changing the starting position of the movement had no consistent effect on the direction of the variable-error major

TABLE 1. *Variable error eigenvalues*

Subject	1st	2nd	3rd	1st	2nd	3rd	1st	2nd	3rd
	Left			Middle			Right		
	A.								
AP	16.8**	7.7*	6.1*	20.0**	8.9*	7.2*	14.2**	8.5**	5.8**
AR	11.1**	6.0**	4.2**	10.6**	5.9**	4.3**	10.6**	5.4**	3.8**
FO	12.7**	7.3	6.8	19.6**	7.8*	5.9*	11.2**	6.1	5.9
MS	6.6**	4.1**	3.2**	6.5**	4.1**	3.1**	7.0**	4.6**	3.2**
SC	10.9**	4.3	3.9	13.8**	4.0	3.4	8.8**	4.1	3.4
SE	6.2**	4.4	3.7	6.3**	4.0	3.8	6.1**	3.9	3.6
	Left			Near			Far		
	B.								
DA	8.9**	6.5**	4.6**	8.0**	4.7	3.8	8.6	7.3	4.6**
FF	11.2**	6.6	5.7	8.6**	6.1**	4.0**	12.2**	7.2**	4.6**
FS	15.6**	6.8*	5.4*	17.8**	5.5	5.0	14.5**	5.5	4.4
JM	7.6**	2.7	2.2	7.5**	2.2**	1.4**	14.1**	3.8*	3.2*

Variable error magnitude (mm) given by the square root of the 3 eigenvalues for the 95% tolerance ellipsoid. Values marked with asterisks are statistically distinct at the $P = 0.01$ (**) or $P = 0.05$ (*) levels.

axis (Fig. 9A). The projected eigenvector for the left starting position (—) passes to the left of the vector for the right starting position (---) in only half of the cases (*subjects AG, FS, and LB*), and in all cases both eigenvectors point toward the head. This is not to say that there is no secondary

effect of the starting hand position. If we project the data into the plane that contains the target position and the two starting positions, we can compute the 2-D variable error as shown in Fig. 9B. The analysis in this plane will be the most sensitive to the imposed changes in starting position. The directions of the major eigenvectors computed in this plane are shown in Fig. 9C. Although for two subjects (*AG* and *JM*) the 2-D eigenvalues were not statistically distinct at the 95% confidence level, the indicated eigenvectors still represent the best estimate of the direction of maximum variation. Considering the data from all subjects, it can be seen that, in general, the eigenvector for the left starting position passes to the left of the corresponding eigenvector for the right starting position (Wilcoxon signed-rank test, $Z = 2.02$, $n = 6$, $P < 0.043$). Looking at the individual, nonsignificant data in this way is analogous to flipping a coin—a single “heads” is not significant in itself, but 9 of 10 heads might indicate a biased coin. Thus an effect of the starting hand position can be detected in the orientation of the distribution of errors, but this effect is minor compared with the strong influence of the direction from the head/eyes to the target.

Left versus right hand

Changing the hand used to perform the movement had no effect on the pattern of variable errors. Figure 10A shows the orientations of the variable-error ellipsoids for the left-near-far paradigm performed with the left hand. These three subjects started each trial from the left starting position. Thus the required movement was the mirror image of the right-hand trials. Vectors for all three workspace locations point toward the head, as was seen for the right hand in Fig. 6. The near and far vectors are parallel, whereas the left vector is rotated with respect to the other two. One subject (*JM*) performed the experiment with the left hand starting from both initial positions. The results, shown in Fig. 10B, are essentially identical for the left (—) and right (---) starting positions. Constant

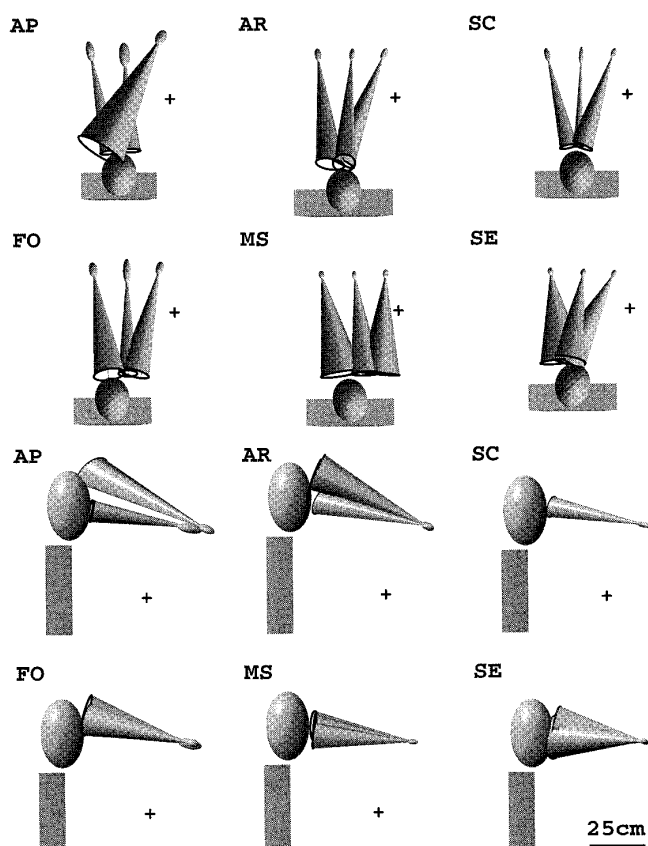


FIG. 5. The 95% confidence cones for the variable-error eigenvector directions shown in Fig. 4. In all cases, the head falls within the confidence cone, whereas the shoulder lies outside.

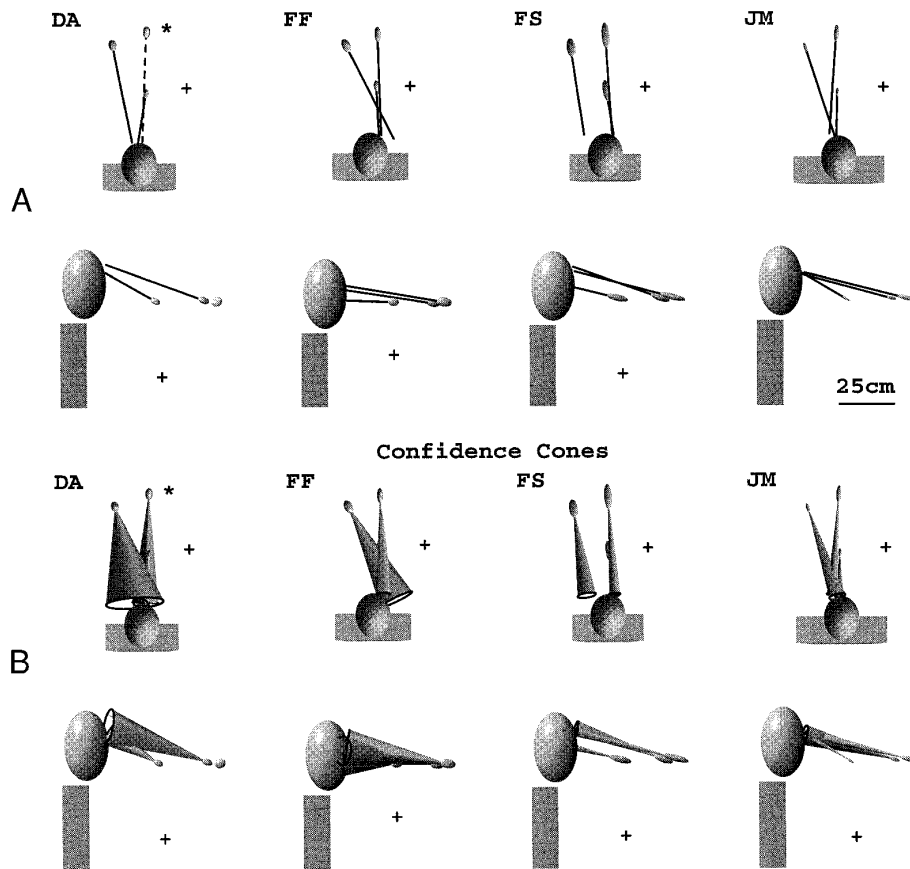


FIG. 6. Variable error for subjects who performed trials to the left, near, and far workspace regions. A: major axis directions projected to the frontal plane passing through the eyes. In 3 of 4 cases, the major axes of the variable-error ellipsoids are parallel for the near and far configurations, whereas the major axis for the left workspace region is rotated with respect to the other 2. For the exception (*subject FS*), all 3 axes are essentially parallel. B: confidence limits for the axes plotted in A. Note that the 1st eigenvalue for the ellipsoid, indicated by an asterisk, is not statistically different from the 2nd at the 95% confidence level. However, the 1st and 2nd eigenvectors define a vertical plane whose intersection with the horizontal is indicated by the dashed line.

errors for *subjects FF* and *JM* (Fig. 11) are comparable with those obtained with the right hand (Fig. 8).

Head rotation

The orientations of both the variable-error ellipsoid and the constant-error vector do not remain aligned with the

body midsagittal plane. Both vectors rotate in response to reorientation of the head. In Fig. 12, a dashed line is drawn between the center of head rotation and the center target position. For trials with the head rotated to the left, both the variable-error major eigenvector and the constant-error vector pass to the left of the dashed midline. Similarly, both vectors pass to the right for the rightward head rotation. The amount of rotation does not, however, correspond exactly to what would be expected from the shift in eye position induced by the head rotation. The confidence cones in Fig. 12 indicate that the rotation of the constant error in the horizontal plane is statistically significant at the 95% confidence level for each of these two subjects. The rotation of the variable-error eigenvector is statistically significant for *subject FF* but not for *subject JM*.

Memory delay

Increasing the duration of the memory delay had little or no effect on the direction of the variable-error major eigenvector. For the two subjects who pointed to targets in the left, middle, and right workspace regions, the major eigenvectors of the variable-error ellipsoids continue to point toward the head (Fig. 13). For the six samples, there is no significant difference between the orientation of the major eigenvector and the orientation of a vector pointing from the eyes to the center target position [$R(2,4) = 1.06$, $P < 0.4263$]. For the subjects who pointed to targets in the far workspace region with two different memory delays (Fig. 14), the difference in the direction of the variable-error ma-

TABLE 2. Constant error magnitudes

Subject	Magnitude			Overshoot		
	Left	Middle	Right	Left	Middle	Right
A.						
AP	27.3	11.3	88.2	24.6	8.5	83.7
AR	13.6	9.3	14.9	2.9	1.8	-1.7
FO	9.4	7.2	17.6	8.3	1.5	9.8
MS	23.8	24.4	23.6	-21.7	-23.9	-21.7
SC	10.3	9.5	14.2	0.4	-5.4	-0.8
SE	10.8	17.1	27.8	-10.6	-16.8	-26.4
Subject	Magnitude			Overshoot		
	Left	Near	Far	Left	Near	Far
B.						
DA	14.9	12.3	28.1	-11.1	-10.5	-27.0
FF	21.0	24.6	41.7	-14.4	23.7	-40.5
FS	30.1	16.2	53.1	-22.8	-7.5	-51.3
JM	29.5	14.6	41.9	-28.7	-13.7	-41.3

Constant error magnitudes (mm), and the degree of overshoot (positive values) or undershoot (negative values), as measured from the head (mm).

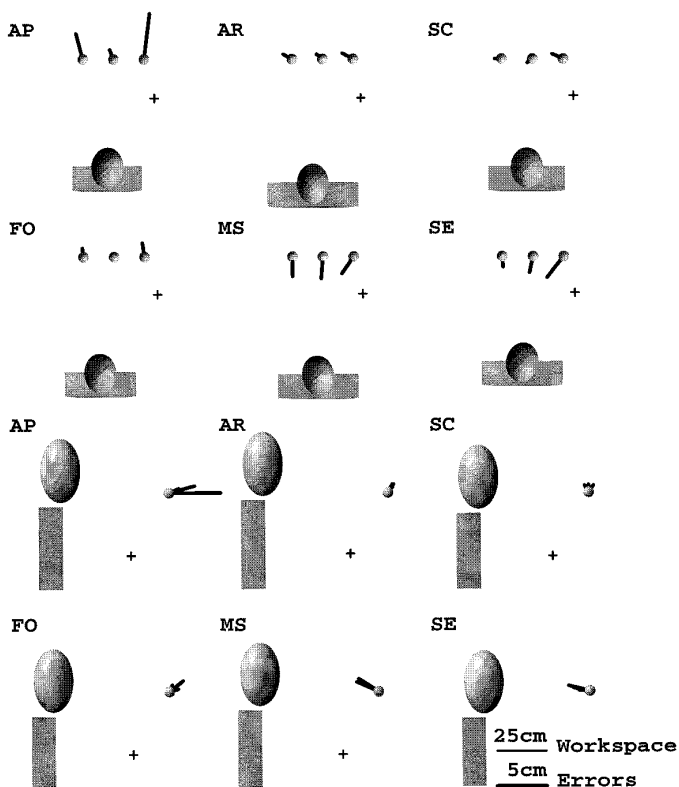


FIG. 7. Constant-error direction and relative magnitude for the left, middle, and right workspace regions. Small spheres: true center target position for each workspace region. Line segments: average constant error for all 9 targets, magnified by a factor of 5 to be visible.

for eigenvector between a short (0.5-s) and long (8.0-s) delay was not statistically significant [$R(2,3) = 6.28$, $P < 0.085$, *subject DA* was excluded from this analysis because the direction of the 1st eigenvector was not statistically significant]. The magnitude of the variable error increased by an average of 3.7 mm in each direction (Fig. 15). To test the significance of the increased variability, we performed an ANOVA on the square roots of the eigenvalues of the variable-error tolerance ellipsoid, with memory delay and eigenvalue rank (1st, 2nd, or 3rd) as independent factors. The memory delay factor had a significant main effect on the average eigenvalue [$F(1,5) = 118.21$, $P < 0.0001$]. There was a significant main effect between the three different eigenvalues [$F(2,10) = 28.42$, $P < 0.001$], where the

difference was significant between the first eigenvalue and the other two, but not between the second and third eigenvalues ($P < 0.0067$ and $P < 0.43$, respectively, Scheffe's *t*-test for post hoc analysis). This confirms our previous analysis that there is no significant anisotropy of variable error in the frontoparallel plane. There was no significant cross-effect of memory delay versus eigenvalue rank [$F(2,10) = 0.37$, $P < 0.70$], indicating that the additive increase of variability, when expressed in terms of the SD, was equal in all three dimensions. Note that the increase was additive, not multiplicative. The ratio of the first to the second eigenvalue decreased with memory delay [$F(1,5) = 11.25$, $P < 0.02$].

DISCUSSION

Specific anisotropies in the distribution of pointing errors provide clear evidence of a viewer-centered reference frame for pointing to remembered targets when vision of the hand is allowed. The axis of maximum variance in the movement endpoints (major axis of the tolerance ellipsoids) passes consistently through the head, very close to midpoint between the eyes. This feature is independent of the location of the target within the workspace, the hand used to perform the movement (left or right), the starting position of the hand, and the orientation of the head during the task. Thus specification of the endpoint position for these movements appears to be related to a viewer-centered, as opposed to an arm-centered, reference frame. In the following discussion we illustrate how binocular distance perception based on eye position or retinal disparity predicts the orientation, but not the shape, of the variable errors. We then show how the control of conjugate eye movements or the fusion of multi-sensory cues can account for the observed endpoint distributions. Finally, we argue that the target location is memorized in a reference frame different from that of the visual input, on the basis of isotropic increases in endpoint variability.

Binocular distance cues—eye position

The tight coupling between the orientation of the variable-error ellipsoid and the presumed orientation of gaze suggests that the anisotropy in 3-D pointing movements might be attributed to variability in the sensory input coming from the binocular visual system. Consider first the computation of target loca-

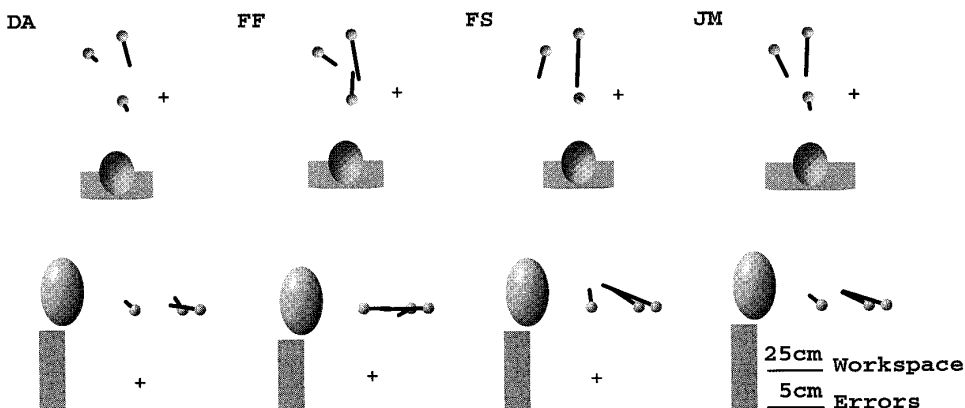


FIG. 8. Constant-error vectors for the left, near, and far configuration, plotted as in Fig. 7.

TABLE 3. *Local target to endpoint transformations*

Subject	M_x	M_y	M_z
AP	1.36 ± 0.05	0.99 ± 0.06	1.06 ± 0.14
AR	1.12 ± 0.03	1.01 ± 0.05	0.60 ± 0.07
FO	1.06 ± 0.04	0.89 ± 0.08	0.56 ± 0.19
MS	0.93 ± 0.02	0.93 ± 0.03	0.67 ± 0.04
SC	1.16 ± 0.02	1.02 ± 0.03	0.99 ± 0.09
SE	1.01 ± 0.02	1.02 ± 0.03	0.75 ± 0.04

Values are regression slopes (means \pm SE) for the correlation of endpoint vs. target position computed separately for each of the 3 Cartesian directions. Data are from 6 subjects for targets in the mid-workspace region. All slopes are significantly different from 0 at $P < 0.0001$.

tion on the basis of the orientation of the two eyes, assuming that the target is bifoveated. Uncompensated eye movements can account for a decreased ability to discriminate differences in positions of visually acquired targets (Matin et al. 1966, 1970). For a given level of random uncertainty in the angular position of each eye, we can calculate the expected variability of the perceived target location as a function of workspace location (see APPENDIX B). The computed workspace variation of this perceptual anisotropy predicts the direction of variable-error ellipsoids seen in our experiments. Uncertainty in depth perception, and thus variability in the pointing distance, will be greater than that of azimuth or elevation for all but the very nearest of target locations (target distances less than half the interocular distance of 6.3 cm).

Variability in eye position signals alone predicts the orientation but not the shape of the pointing error distribution. For a target located 60 cm from the eyes, left/right and up/down variability should be 20 times smaller than the variability in depth. Comparison of the first and second eigenvalues from our experiments indicate a factor closer to 2 or 3 to 1. We offer two possible explanations for this discrepancy.

VERGENCE VERSUS VERSIONAL EYE MOVEMENTS. The preceding analysis assumes that variability in eye position sense was stochastically independent for each of the two eyes. If, instead, uncompensated eye movements tend to be coupled, with a differential in the control of conjugate versus disjunc-

tive eye movements, the structure of the sensory input variability will be altered. It is generally accepted that conjugate eye movements and vergence are controlled by separate brain stem circuits, although these two systems are evidently coordinated (Mays and Gamlin 1995). It is therefore reasonable to expect that eye position fluctuations might covary. Mathematically, this means that the covariance matrix for eye position information will no longer be diagonal with equal eigenvalues. The anisotropy in the eye position variance will change the shape of the transformed output variance (see APPENDIX B). A finer control of vergence versus version eye movements would decrease the variability of the final pointing depth with respect to variability in the tangent plane.

Van Eë and Erkelens (1996) propose a different mechanism that might explain an apparently greater stability for visual depth perception. Displacements of entire half-images of a random dot stereogram induce vergence movements in the eyes but limited perceptions of changes in depth (Erkelens and Collewyn 1985a,b; Regan et al. 1986). Changes in relative disparity within the stereogram, on the other hand, elicit strong perceptions of depth changes. Furthermore, fast side-to-side head movements or pressing against the eyeball generate vergence changes that are not perceived as changes in target depth (Steinman et al. 1985). Van Eë and Erkelens have hypothesized that movements of the entire retinal image are ignored or attenuated by the depth perception system, because such retinal shifts are ambiguously related either to changes in object distance or to variations in eye or head position. To explain the results of the current study in this context, however, it must be shown that slip of an entire retinal image induces perceptions of change of target direction but not of target depth. Sustained passive rotation of one eye can indeed induce changes in ocular alignment and concomitant changes of perceived target direction (Gauthier et al. 1994).

FUSION OF MULTIPLE SENSORY CUES. Under our experimental conditions, subjects have more cues than just the convergence of the eyes with which to estimate the target distance. Relative disparity between the target and fixation lights

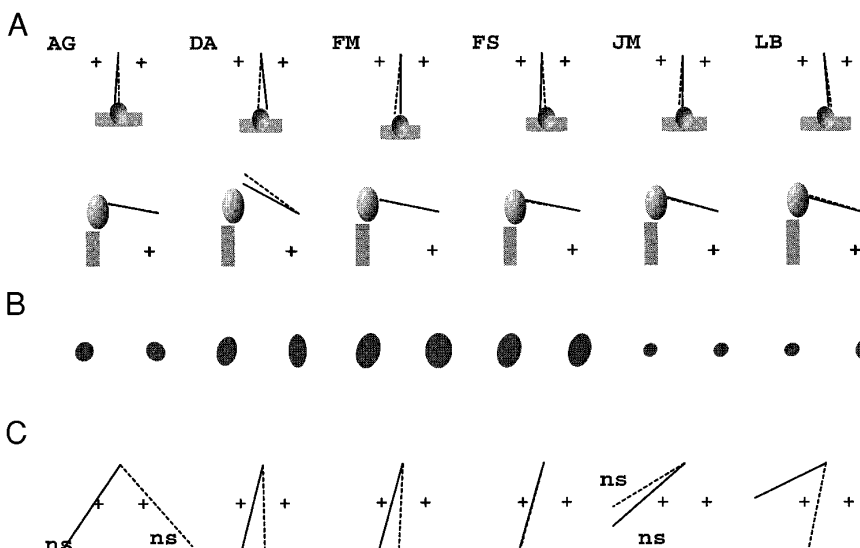


FIG. 9. Comparison of variable-error orientation for the left vs. right starting positions. A: 3-dimensional (3-D) major axis directions for the left (—) and right (---) starting positions to a single workspace region (far region). B: 2-D variable-error ellipses computed in the plane containing the 2 starting positions and the center target location. C: directions of the 2-D variable-error major axes. Across subjects, the best estimate of 2-D variable error rotates with the starting position, although when taken individually the major eigenvalues for the axes marked ns are not statistically different from the corresponding 2nd eigenvalue at the 95% confidence level.

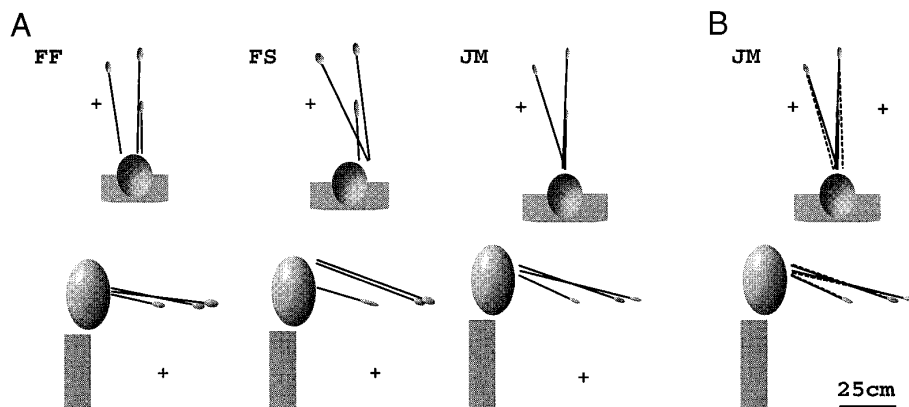


FIG. 10. Variable-error orientation for the left hand. A: 3 subjects using the left hand, starting from the left hand starting position. Results are nearly identical to movements with the right hand from the right side (Fig. 6). B: subject JM performed the experiment with the left hand, starting from both the left (—) and right (---) starting positions. Results are indistinguishable for the 2 starting positions.

might provide one such extra cue, as would the absolute disparity of the observed finger position near the end of the movement as the subject fixates the remembered target location. For these experimental conditions, both absolute and relative disparity is useful in the acquisition of the target location, whereas in the comparison of the finger position to the remembered target position, only absolute disparity cues are available in the absence of a visual reference point. Relative disparity provides a much more powerful indication of target depth that is on the order of 10 times more precise than absolute depth cues (Westheimer 1979). Foley (1976) measured discriminability in a visual task with the use of successive presentation of two stimuli located ~ 63 cm from the viewer. Using a forced-choice, staircase paradigm, Foley found discriminability thresholds on the order of 4–10 minarc for both depth and vernier (azimuth) displacements at an interstimulus interval of 1 s. A 5-min SD for absolute disparity measurements would result in a 12-mm SD in the depth direction. This is in agreement with the average magnitude of the major eigenvalues for the 3-D SDs calculated in our experiment for targets at a comparable distance. One might conclude, therefore, that the variable error seen in our experiments arises from the comparison of the fingertip position and the remembered target position at the end of the movement rather than from variability in the visual acquisition of the target position.

Retinal disparity cues alone are not sufficient to explain the shape of the covariance ellipsoids seen in our experiments. The computation of depth and direction based on absolute disparity has the same form as that of vergence.

The transformation of equal variances for monocular disparities into Cartesian coordinates also results in a 20:1 ratio of covariance eigenvalues.

Accommodation provides an additional cue as to the depth of the target location and final fingertip position. Blur in the retinal image of the fingertip as the subject fixates the remembered target position can indicate when the fingertip is at the proper depth. For accommodation to be useful in reducing variable error at the endpoint, it must provide information that is independent from vergence signals. It is known that vergence can be triggered by blur-driven accommodation (Jiang 1996; Mays and Gamlin 1995). Conversely, the vergence controller can initiate an accommodative response. Thus dynamic vergence and accommodation signals would appear to be correlated. However, in addition to the phasic responses, tonic components are present in this cross-linked system. Accommodative and vergence eye movements in darkness are thought to represent tonic accommodation and tonic vergence, respectively. Current models of this system indicate that the cross-links are driven only by the phasic control elements, the tonic elements being located after the cross-coupling (Jiang 1996; Schor 1992). Accordingly, the resting position of accommodation and vergence in the absence of adequate stimulation should be independent of each other (Owens and Leibowitz 1980).

Because blur is related primarily to object depth, accommodation is one visual cue that might reduce distance variance without affecting directional accuracy. Because tonic accommodation and vergence cues are independent, the integration of vergence and accommodation information reduces

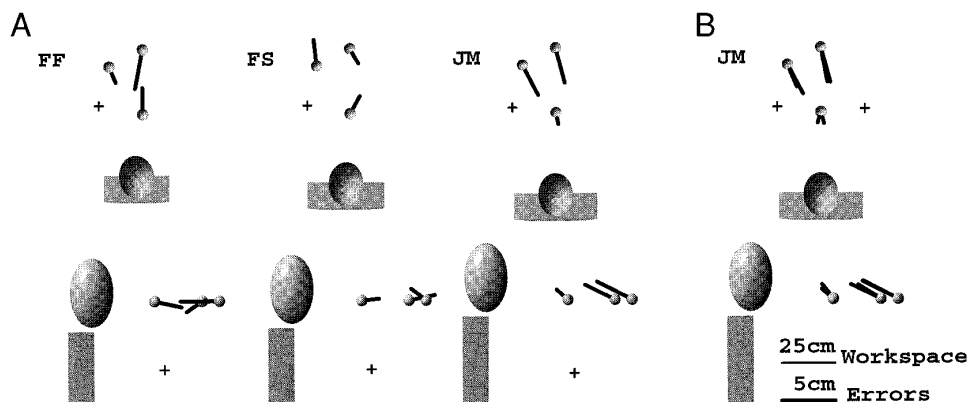


FIG. 11. Constant error for trials performed with the left hand from the left starting position (A) and from both the left and right starting positions (B).

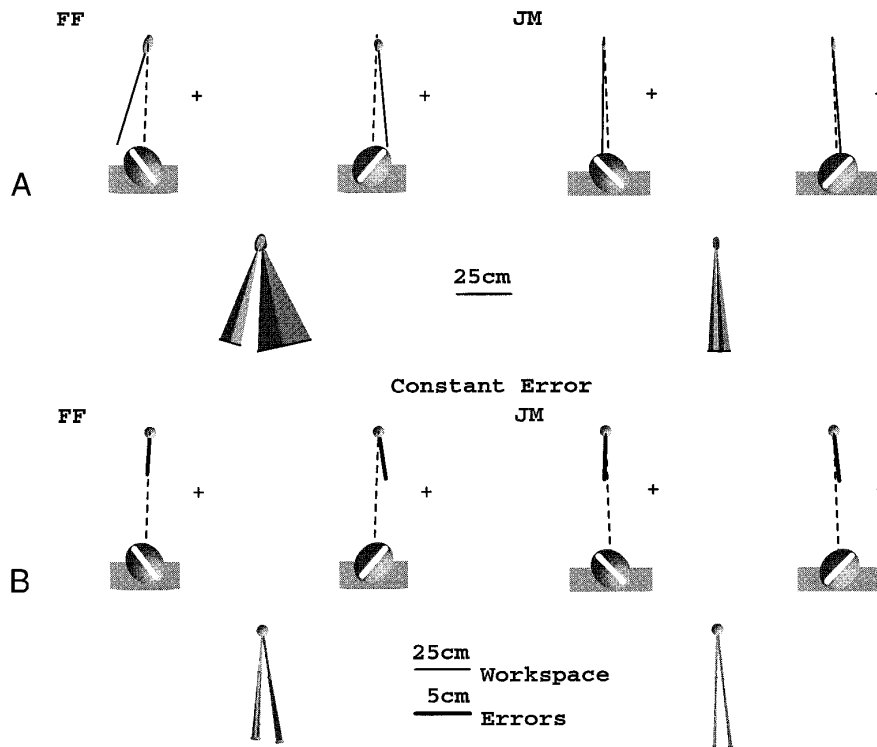


FIG. 12. Variable error (A) and constant error (B) for pointing trials performed with the head turned to the left or right. White bar on the head: direction of head rotation. — — —, midline as defined by the center of the head and the center of the far target region. Cones at *bottom middle* of each panel: overlaid 95% confidence cones for the variable-error (A) and constant-error (B) estimates computed in the horizontal plane for each head orientation. Both the variable error and the constant error rotate to the left for a leftward rotation of the head and to the right for a rightward head rotation.

the net variance in the estimated distance. Note that, unlike vergence, blur is ambiguous for the direction of depth. Although blur may not indicate the direction of an error in depth, minimizing blur can still serve to reduce variability in distance estimates.

It seems likely that subjects combined multiple sensory cues in the performance of this particular pointing task. Gogel (1969, 1972) has proposed a model of distance perception in which different monocular and binocular cues combine to form an estimate of target distance. Anderson (1974) has proposed a quantitative model in which the target distance estimate is a weighted sum of available cues and the specific distance effect. Foley and Held (1972) compared radial pointing under two conditions: with multiple distance cues and under carefully controlled vergence-only conditions, finding, as expected, greater accuracy under the

multicue condition. The magnitude of the variable error for our experiments corresponds better to the variability observed in the multicue condition of Foley and Held. Neural activity for cells in area LIP of monkey parietal cortex varies according to target depth (Gnadt and Mays 1995). Firing rates for these cells are modulated by both changes in stimulus blur and changes of vergence angle or absolute disparity. Thus we have both psychophysical and physiological evidence for the integration of vergence, disparity, and accommodation signals within the CNS.

Egocentric ocular inputs versus allocentric visual cues

In a study of visually guided pointing to a remembered target position (condition with lights on), Soechting et al. (1990) also concluded that subjects use a head-centered coordinate system to perform the task. They interpreted these results on the basis of the fact that subjects could align the target with visual references in the background. Under our experimental conditions, viewer-centered variable errors were observed despite the lack of visual cues in the background. Thus it would seem that the anisotropy observed in pointing variability reflects the anisotropy in the treatment of egocentric ocular information rather than reliance on allocentric visual cues.

Distortions induced by coordinate transformations

We have argued that the pattern of variable errors arises from the transformation of ocular information into an estimate of 3-D position. Furthermore, we have proposed that the discrepancy between the predicted 20:1 and observed 2:1 ratio of covariance eigenvalues be explained by the reduction of depth-related variance through coupled eye move-

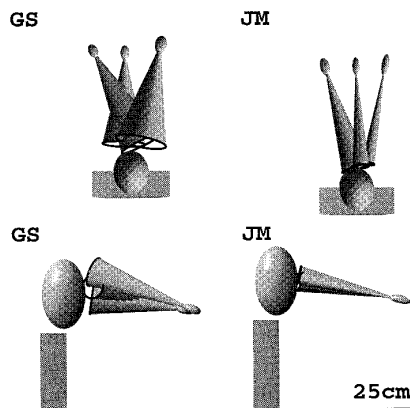


FIG. 13. Variable-error orientation for pointing trials with a long (5.0-s) memory delay period. Major eigenvectors of the variable-error ellipsoids point toward the head.

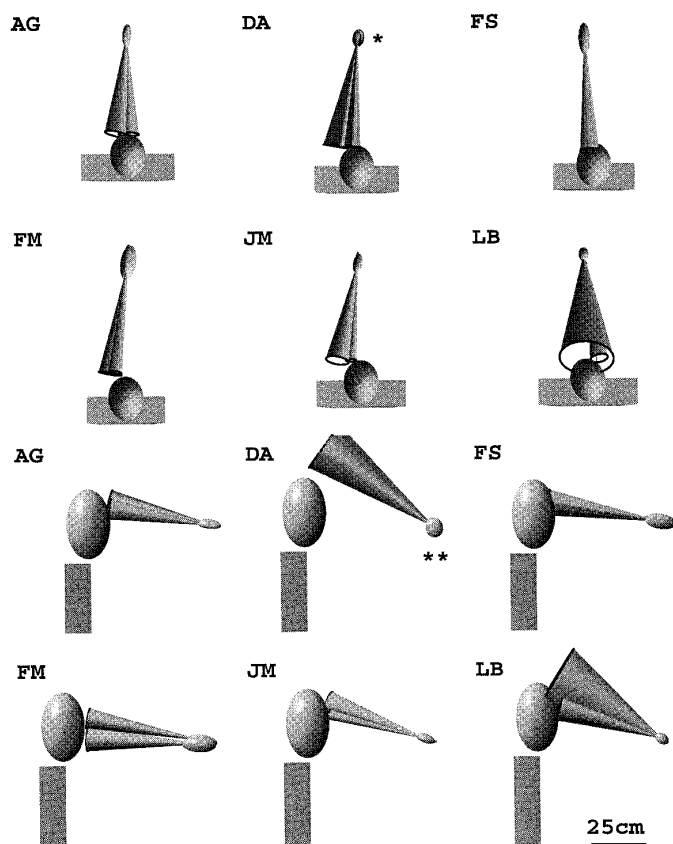


FIG. 14. Variable-error orientations and 95% confidence cones for long (8.0-s) and short (0.5-s) memory delays intermixed within the same block of trials. Eigenvectors of the covariance matrix point toward the head for both delays. For *subject DA*, the 2 major 3-D eigenvalues were not distinct for the long delay. First and 2nd eigenvectors lie in a parasagittal plane passing through the head. Overhead view: 2-D eigenvector in the horizontal plane (*); lateral view includes only the eigenvector direction for the short delay (**).

ments and/or integration of multiple visual and oculomotor cues. An additional explanation for the observed ratio must be considered. In a pointing task the CNS transforms sensory input about the target location in space into a motor output that achieves the final pointing position, passing perhaps through an intermediate representation of the target location. If the transformation is exact, the distribution of pointing errors expressed in Cartesian coordinates will be unaffected by the sensorimotor transformation. On the other hand, if

the coordinate transformations are inexact, distortions will be observed in the mapping of target to finger positions.

Soechting and colleagues have proposed just such a model for the transformation of perceived target position to motor output. They postulate that the CNS uses a linear approximation to transform target distance, azimuth, and elevation into shoulder and elbow angles (Soechting and Flanders 1989b). They base this model on systematic undershoots in pointing to remembered targets. Soechting's model predicts the compression of target depth information seen in their experiments.

In a similar vein, Foley (1980) has reviewed extensively the literature on binocular depth perception and finds that subjects tend to misjudge the true distance of a visually perceived target irrespective of the reporting procedure used (verbal response, pointing, etc.). A linear relationship between actual and perceived target vergence angle with slope less than unity fits the available data well. Although the slopes and intercepts of the fitted relationships would predict overshoots, instead of undershoots, for reachable targets, this model of sensory perception also predicts a compression of data in the depth dimension.

An inexact transformation between sensory or motor variables would affect both the variable and constant errors produced in a pointing task. We do not see systematic undershoots or overshoots in pointing to visually remembered targets across different workspace regions. Thus we have no evidence for a globally inaccurate transformation of perceived target location. This may be due to the fact that subjects reached to a relatively small region of the workspace for a given set of trials. Although a specific approximation to a sensorimotor transformation may be employed, subjects seem to be able to calibrate the transformation to achieve good accuracy for a small workspace region.

On comparing targets within a single workspace region, we do see a relative compression of the responses in distance with respect to the presented target positions. A linear regression of target versus response depth reveals a slope that is significantly <1 , in contrast to the near-unity slopes seen for regressions of target versus response azimuth or elevation (Table 3). This compression of the responses in depth may be attributed to a range effect (Brown et al. 1948) or specific distance tendency (Gogel 1969) rather than to a specific approximation in a sensorimotor transformation. In any case, the magnitude of the effect is not sufficient to account for the eccentricity of the variable-error ellipsoids. A compression

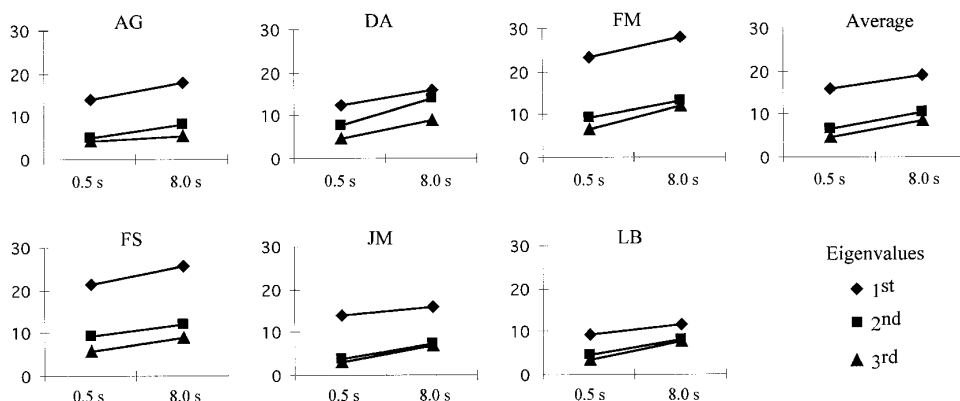


FIG. 15. Variable-error magnitude as a function of memory delay. Magnitudes are expressed in mm as the square root of the 3 eigenvalues of the tolerance ellipsoid. Variability of final finger positions increases additively by an equal amount in all directions.

factor of 0.6 would reduce the eigenvalue ratio from 20:1 to 12:1 instead of the observed 2:1 ratio.

As noted in the preceding text, we observed no consistent pattern of errors related to a specific inaccuracy in the transformation from the visual input to the motor output. Gordon et al. (1994), on the other hand, based their arguments for separate processing of movement extent and direction on patterns of variable error observed in their experiments independent of constant errors introduced by the sensorimotor transformation. The lack of strong evidence in our data for such a hand-centered reference frame may be accounted for by differences in experimental conditions. A recent study by Desmurget et al. (1997) has shown that movement kinematics and variable-error distributions can depend on whether the movement is completely unconstrained (as in our study) or whether the movement is executed in compliance with a physical constraint (as for the experiments performed by Gordon et al. 1994). A second difference between these experiments concerns the visual conditions. In the current study, subjects could see their hands during the course of the movement. Thus the question remains as to whether visually guided updates during the course of the movement might alter the initial visuomotor transformation.

Memory storage

We have argued that the anisotropy in variable errors for pointing arises from the binocular estimation of target and finger position. For the visually guided movements studied here, there is no need to postulate any other representation of the positions within the CNS. The brain could simply compare the input parameters (vergence angle, disparity, and accommodation) of the visually perceived finger position with the remembered target parameters expressed in the same terms. Variability of the inputs will manifest itself as anisotropy for depth versus direction at the output, but this does not mean that the CNS represents the target position explicitly in terms of a spherical coordinate system.

Does the CNS indeed memorize the target location in the intrinsic coordinates of the input, or are the data somehow transformed into another internal representation? For pointing trials with a 5- to 8-s memory delay, the variability of responses increased equally in all three dimensions with respect to a memory period of only 0.5 s. Discriminability thresholds have also been shown to increase as a function of memory delay for a variety of unidimensional stimuli (Kinchla and Smyzer 1967). Specifically, it was found that decreases in discriminability with increasing time delays can be modeled by a diffusional process in which the variance of the remembered stimulus value increases linearly with time. The fact that the size of the variable-error tolerance ellipsoid increased isotropically in our experiments indicates that the storage of the target position may be carried out in transformed coordinates. In fact, the same transformation that generates a radial anisotropy in depth for the perceived target position would apply to increases in variability induced by the prolonged memory delay (see APPENDIX A). The observed changes in variable error would be inconsistent with the model of memory decay of Kinchla and Smyzer if the memorized target position were stored in retinal or oculomotor coordinates. Furthermore, the observed increases

in variable error do not correspond to the increases in discriminability thresholds for a purely visual task. Foley (1976) observed that the ratio of depth and vernier discriminability thresholds, expressed in terms of visual arc, remained constant, whereas both increased as a function of interstimulus delay. Thus, although Kinchla's model can adequately explain Foley's data in terms of retinal or oculomotor coordinates, such a description cannot fully account for the pointing data. Indication of a memorized target position through reaching, as opposed to a visual judgment of target locations, seems to modify the pattern of variable errors and thus might indicate a difference in the memory encoding for these two different tasks.

Patterns of eye movement errors to memorized targets cannot explain the pointing errors observed in our experiments. Monkeys and humans demonstrate systematic errors when performing memory saccades, fixating consistently above the actual target position (Gnadt et al. 1991; White et al. 1993). For memory saccades, there is a dissociation between the patterns of constant and variable errors—the magnitude of constant errors reaches a stable maximum after only 400 ms, whereas variable-error magnitude rises monotonically over ≥ 2.4 s. Ocular drift during the dark fixation period cannot explain constant errors observed for memory saccades (White et al. 1993). In our experiment, subjects performed saccades to the target while it was still visible. Thus we cannot expect to relate errors in pointing directly to error in the performance of memory saccades. However, pointing errors might be related to eye position drift if subjects were merely comparing the remembered retinal image of the target with the observed position of the fingertip. The data do not confirm this hypothesis. Upward and leftward drift in eye position would result in a pattern of constant errors upward and to the left, with an elongation of the variable error in the same direction. We see no such consistent pattern of errors for pointing with the finger to a remembered target.

The isotropic increase of the tolerance ellipsoids as a function of memory delay suggests that the target location may be memorized in a Cartesian reference frame. Such an encoding of the target position would require the combination of depth and directional cues before the storage of the target position. Cross-coupling of distance and direction information has been observed for cells within primate parietal area LIP. Certain cells in this area signal actual or intended changes in eye position in the absence of retinal stimulation, as seen in the production of memory saccades (Gnadt and Andersen 1988; Gnadt and Mays 1995). The authors have argued that these neurons encode their activity in motor spatial parameters, with motor fields that are shaped according to a 2-D Gaussian function in the frontoparallel plane (directional tuning) and a broad sigmoid function in depth (Gnadt and Mays 1995). Irrespective of whether or not this cortical area is directly involved in the control of manual pointing, these eye-movement-related cells provide an example of the integration of depth and direction information within the CNS. The sensitivity of these cells to depth may provide a mechanism by which the CNS can transform spherically referenced sensory information into a spatially isotropic representation.

The memorization of target location in a Cartesian ref-

erence frame is an attractive hypothesis, but one that remains speculative at this point. Differential increases in variance for independent input cues such as vergence and accommodation might explain why the shape of the overall variance does not change as expected, although it seems unlikely that the increase in the different channels would be matched so as to precisely cancel the unequal increase in the transformed variability. Similarly, just as we have argued above that coupled eye movements might affect the shape of the variable error, an increase in the correlation of movements between the eyes for longer delays might also explain the less-than-expected increase in depth variability. Although further evidence is needed, the hypothesis of an isotropic internal representation nevertheless seems worth pursuing.

Conclusions

Errors for pointing to remembered targets are distinct between target distance and direction from the eyes. This result is independent of movement starting position, effector hand, workspace location, and head orientation, demonstrating a viewer-centered anisotropy for the reproduction of the target positions. Analysis of the variable error indicates that the pattern of errors most probably arises from the inherent geometric properties of the binocular perception of distance and direction. Isotropic increases in variability with memory delay nevertheless suggest that spatial memory is carried out in an internal representation that does not simply mirror the retinal and ocular sensory signals of the visually acquired target location.

APPENDIX A: TRANSFORMATION OF VARIANCE

As information is passed from one coordinate frame to another, random noise in the input variable will be transformed into variability in the output. If the transformation is known, the form of the output variability can be computed from the form of the input variance. In this section we derive the equations for the transformation of variance between coordinate systems.

Let x be an n -dimensional vector representing the input information, y be the m -dimensional output variable, and $y = L(x)$ indicate the transformation of information between coordinate frames. Furthermore, let x be a random variable with mean x_0 and variance S_δ . S_δ need not necessarily be diagonal. That is, the components of x are not necessarily independent. For relatively small variations of the input variable x , the distribution of the output variable y is computed as follows

$$x_i = x_0 + \delta_i \quad (A1)$$

where δ_i is a randomly distributed vector with zero mean and variance S_δ . For small displacements from x_0 , the corresponding value for y is approximately

$$y_i = L(x_0 + \delta_i) \quad (A2)$$

$$\cong L(x_0) + J(x_0)\delta_i \quad (A3)$$

$$\cong y_0 + J(x_0)\delta_i \quad (A4)$$

where $J(x_0)$ is the Jacobian matrix of the transformation $L(x)$ evaluated at $x = x_0$

$$J(x) = \begin{bmatrix} \frac{\partial y^1}{\partial x^1} & \cdots & \frac{\partial y^1}{\partial x^n} \\ \vdots & \ddots & \vdots \\ \frac{\partial y^m}{\partial x^1} & \cdots & \frac{\partial y^m}{\partial x^n} \end{bmatrix} \quad (A5)$$

The distribution of the variable y is given by

$$S_y = \sum_i (y_i - y_0)(y_i - y_0)^T \quad (A6)$$

$$= \sum_i \left[y_0 + J(x_0)\delta_i - y_0 \right] \left[y_0 + J(x_0)\delta_i - y_0 \right]^T \quad (A7)$$

$$= \sum_i J(x_0)\delta_i \delta_i^T J^T(x_0) \quad (A8)$$

$$= J(x_0)S_\delta J^T(x_0) \quad (A9)$$

The addition of variance in the input variable x results in an increase in variance for the output y . The change in variance for the two variables is also related by the Jacobian matrix

$$x'_i = x_0 + \delta_i + \eta_i \quad (A10)$$

where η_i has zero mean and variance S_η

$$S'_x = S_\delta + S_\eta \quad (A11)$$

$$S'_y = J(x_0)[S_\delta + S_\eta]J^T(x_0) \quad (A12)$$

$$= S_y + J(x_0)S_\eta J^T(x_0) \quad (A13)$$

Thus the additive change in output variance ΔS_y is related to the additive change in input variance S_η

$$\Delta S_y = J(x_0)S_\eta J^T(x_0) \quad (A14)$$

Similarly, a scaling of the input variance will result in a scaling of the output variance

$$S'_x = rS_\delta \quad (A15)$$

$$S'_y = J(x_0)[rS_\delta]J^T(x_0) \quad (A16)$$

$$= rS_y \quad (A17)$$

and the additive increase of the output variance will have the same shape as the original transformed variance

$$\Delta S_y = (r - 1)S_y \quad (A18)$$

In both cases, an isotropic increase in variance at the input will cause an increase of variance at the output that is shaped by the coordinate transformation.

APPENDIX B: TRANSFORMATION OF RANDOM NOISE IN OCULOMOTOR SIGNALS TO CARTESIAN VARIABILITY

Random noise in retinal and oculomotor signals will generate variability in visually perceived estimates of spatial locations. In this section we derive expressions for computing the variability of spatial estimates expressed in Cartesian coordinates on the basis of estimates of the variance for the oculomotor inputs.

Eye position signals corresponding to a foveated target can be transformed directly into a perceived Cartesian target position

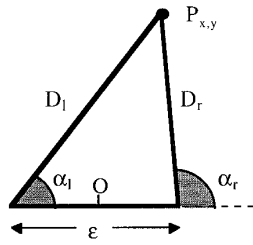


FIG. A1 Definition of terms for the calculation of Cartesian target position (x, y) from binocular information, where α_l and α_r are the angular position of the target with respect to the eye and ϵ is the interocular distance.

where P is the target position, α_l , α_r are the eye orientations, and ϵ is the interocular distance (Fig. A1). From the law of sines

$$\frac{D_r}{\sin \alpha_l} = \frac{\epsilon}{\sin (\alpha_r - \alpha_l)} \quad (A19)$$

From trigonometry and substitution

$$x = D_r \cos \alpha_r + \frac{\epsilon}{2} \quad (A20)$$

$$= \frac{\epsilon \sin \alpha_l \cos \alpha_r}{\sin (\alpha_r - \alpha_l)} + \frac{\epsilon}{2} \quad (A21)$$

$$y = D_r \sin \alpha_r \quad (A22)$$

$$= \frac{\epsilon \sin \alpha_l \sin \alpha_r}{\sin (\alpha_r - \alpha_l)} \quad (A23)$$

Small displacements of eye position give rise to small displacements of the perceived target X - Y position. These displacements are related by the Jacobian matrix of the transformation

$$J(\alpha_l, \alpha_r) = \begin{bmatrix} \frac{\partial x}{\partial \alpha_l} & \frac{\partial x}{\partial \alpha_r} \\ \frac{\partial y}{\partial \alpha_l} & \frac{\partial y}{\partial \alpha_r} \end{bmatrix} \quad (A24)$$

$$\frac{\partial x}{\partial \alpha_l} = \frac{\epsilon \cos \alpha_r}{\sin^2 (\alpha_r - \alpha_l)} [\sin (\alpha_r - \alpha_l) \cos \alpha_l + \sin \alpha_l \cos (\alpha_r - \alpha_l)] \quad (A25)$$

$$\frac{\partial y}{\partial \alpha_l} = \frac{\epsilon \sin \alpha_r}{\sin^2 (\alpha_r - \alpha_l)} [\sin (\alpha_r - \alpha_l) \cos \alpha_l + \sin \alpha_l \cos (\alpha_r - \alpha_l)] \quad (A26)$$

$$\frac{\partial x}{\partial \alpha_r} = -\frac{\epsilon \sin \alpha_l}{\sin^2 (\alpha_r - \alpha_l)} [\sin (\alpha_r - \alpha_l) \sin \alpha_r + \cos \alpha_r \cos (\alpha_r - \alpha_l)] \quad (A27)$$

$$\frac{\partial y}{\partial \alpha_r} = \frac{\epsilon \sin \alpha_l}{\sin^2 (\alpha_r - \alpha_l)} [\sin (\alpha_r - \alpha_l) \cos \alpha_r - \sin \alpha_r \cos (\alpha_r - \alpha_l)] \quad (A28)$$

The variance S_{xy} of the perceived target position can be calculated from the variance of the perceived eye positions (see APPENDIX A)

$$S_{xy} = J(\alpha_l, \alpha_r) S_\alpha J^T(\alpha_l, \alpha_r) \quad (A29)$$

where S_α represents the variance of the left and right eye positions. For a given target position (X, Y) , the eye orientations can be computed by

$$\begin{aligned} \alpha_r &= \tan^{-1} \left(\frac{P_y}{P_x - \frac{\epsilon}{2}} \right) \\ \alpha_l &= \tan^{-1} \left(\frac{P_y}{P_x + \frac{\epsilon}{2}} \right) \end{aligned} \quad (A30)$$

and the predicted covariance matrix S_{xy} can be computed from a given eye position variance S_α with the use of Eq. A24–A29.

Predicted cartesian variances

Using these calculations, we can predict the shape of pointing errors expressed in Cartesian coordinates that would be evoked by variability in the oculomotor system. This calculation makes no assumptions about the underlying neural processes that perform the transformation. In fact, this computation predicts the pointing errors for the case where the subject simply matches the retinal position of the finger to the remembered retinal position of the target, with all variance arising from uncompensated eye movements. Note, however, that similar errors will be produced at the endpoint for any sensorimotor transformation provided that the source of the information is eye position and that the transformation accurately reproduces the 3-D target position.

We first consider the assumption that uncompensated eye movements are stochastically independent between the two eyes

$$S_{xy} = J(\alpha_l, \alpha_r) \begin{bmatrix} \sigma_l & 0 \\ 0 & \sigma_r \end{bmatrix} J^T(\alpha_l, \alpha_r) \quad (A31)$$

where σ_l and σ_r represent the variance of the perceived eye position for the left and right eyes, respectively. We cannot calculate the absolute Cartesian variance of the perceived target position without knowing the values of σ_l and σ_r . We can estimate the shape and direction of S_{xy} , however, by assuming that σ_l equals σ_r . For these examples, we use an eye position SD of 5 minarc, which corresponds to apparent discrimination thresholds for human subjects (see text). Note, however, that the shape and orientation of the Cartesian covariance is not affected by the absolute value of this parameter. The computed Cartesian covariance matrix S_{xy}^* will be related to the true covariance S_{xy} by a scale factor, and the two matrices will have the same eigenvectors and the same eigenvalue ratio. For a target located straight ahead at a distance of 600 mm and an interocular distance of 60 mm, the transformed eye position variance is

$$S_{xy} = \begin{bmatrix} 0.38 & 0.0 \\ 0.0 & 153.1 \end{bmatrix}$$

The square roots of the eigenvalues of the Cartesian variance indicate the magnitude of the variability (SD) in millimeters along each major axis. The ratio of the SDs indicates the shape of the variance independent of size. The above Cartesian variance is diagonal, with an SD ratio of 20:1, indicating that the Cartesian SD resulting from equal variances in the two eyes will be 20 times greater in the depth versus lateral directions.

In a second example, we estimated the Cartesian distribution of errors on the basis of the assumption that disjunctive eye movements are more finely controlled than conjugate eye movements. To illustrate, we assumed an arbitrary ratio of 2:1 for the SD of version versus vergence eye movements. In this case the eye position variance will have the form

$$S_\alpha = \begin{bmatrix} 1.5\alpha_v & 0.5\alpha_v \\ 0.5\alpha_v & 1.5\alpha_v \end{bmatrix}$$

where α_v is the SD of disjunctive (vergence) eye movements. Setting $\alpha_v = 5$ min, the resulting Cartesian variance is

$$S_{xy} = \begin{bmatrix} 1.53 & 0.0 \\ 0.0 & 153.1 \end{bmatrix}$$

giving a Cartesian SD ratio of 10:1. Note that uncompensated head movements would have a similar effect. Expressed in terms of absolute gaze orientation, head rotations affect the conjugate orientation of the eyes without affecting vergence.

The authors thank M. Carrozzo, F. Migliore, D. Angelini, and L. Bianchi for help with the experiments and G. Baud-Bovy for assistance with the statistical equations. We also thank M. Giacomelli and MES s.p.a for luminance measurement equipment and technical assistance.

This work was supported in part by grants from the Italian Health Ministry, the Italian Space Agency, and the Human Frontier Science Program.

Address for reprint requests: J. McIntyre, Istituto Scientifico S. Lucia, via Ardeatina 306, 00179 Rome, Italy.

Received 17 December 1996; accepted in final form 14 May 1997.

REFERENCES

- ANDERSON, N. H. Algebraic models in perception. In: *Handbook of Perception*, edited by E. C. Carterette and M. P. Friedman. New York: Academic, 1974, vol. 2, p. 167–175.
- BERKINBLIT, M. B., FOOKSON, O. I., SMETANIN, B., ADAMOVICH, S. V., AND POIZNER, H. The interaction of visual and proprioceptive inputs in pointing to actual and remembered targets. *Exp. Brain Res.* 107: 326–330, 1995.
- BOCK, O. Contributions of retinal versus extraretinal signals towards visual localization in goal-directed movements. *Exp. Brain Res.* 64: 476–482, 1986.
- BOCK, O. AND ECKMILLER, R. Goal-directed arm movements in absence of visual guidance: evidence for amplitude rather than position control. *Exp. Brain Res.* 62: 451–458, 1986.
- BOOKSTEIN, F. L. Error analysis, regression and coordinate systems (commentary to Flanders et al.). *Behav. Brain Sci.* 15: 327–328, 1992.
- BROWN, J. S., KNAUFT, E. B., AND ROSEBAUM, G. The accuracy of positioning reactions as a function of their direction and extent. *Am. J. Psychol.* 61: 167–182, 1948.
- COLLEWIJN, H. AND ERKELENS, C. J. Binocular eye movements and the perception of depth. In: *Eye Movements and Their Role in Visual and Cognitive Processes*, edited by E. Kowler. Amsterdam: Elsevier, 1990, p. 213–260.
- DARLING, W. G. AND MILLER, G. F. Transformations between visual and kinesthetic coordinate systems in reaches to remembered object locations and orientations. *Exp. Brain Res.* 93: 534–547, 1993.
- DESMURGET, M., JORDAN, M., PRABLANC, C., AND JEANNEROD M. Constrained and unconstrained movements involve different control strategies. *J. Neurophysiol.* 77: 1644–1650, 1997.
- DIEM, K. (Editor). *Tables Scientifiques*. Basel: Geigy, 1963, p. 184.
- ERKELENS, C. J. AND COLLEWIJN, H. Motion perception during dichoptic viewing of moving random-dot stereograms. *Vision Res.* 25: 583–588, 1985a.
- ERKELENS, C. J. AND COLLEWIJN, H. Eye movements and stereopsis during dichoptic viewing of moving random-dot stereograms. *Vision Res.* 25: 1689–1700, 1985b.
- FISK, J. D. AND GOODALE, M. A. The organization of eye and limb movements during unrestricted reaching to targets in contralateral and ipsilateral space. *Exp. Brain Res.* 60: 159–178, 1985.
- FLANDERS, M., TILLERY, S.I.H., AND SOECHTING, J. F. Early stages in a sensorimotor transformation. *Behav. Brain Sci.* 15: 309–362, 1992.
- FOLEY, J. M. Error in visually directed manual pointing. *Percept. Psychophys.* 17: 69–74, 1975.
- FOLEY, J. M. Successive stereo and vernier position discrimination as a function of dark interval duration. *Vision Res.* 16: 1269–1273, 1976.
- FOLEY, J. M. Binocular distance perception. *Psychol. Rev.* 87: 411–435, 1980.
- FOLEY, J. M. AND HELD, R. Visually directed pointing as a function of target distance, direction and available cues. *Percept. Psychophys.* 12: 263–268, 1972.
- GAUTHIER, G. M., VERCHER, J. L., AND ZEE, D. S. Changes in ocular alignment and pointing accuracy after sustained passive rotation of one eye. *Vision Res.* 34: 2613–2627, 1994.
- GNADT, J. W. AND ANDERSEN, R. A. Memory related motor planning activity in posterior parietal cortex of macaque. *Exp. Brain Res.* 70: 216–220, 1988.
- GNADT, J. W., BRACEWELL, M., AND ANDERSEN, R. A. Sensorimotor transformation during eye movements to remembered visual targets. *Vision Res.* 31: 693–715, 1991.
- GNADT, J. W. AND MAYS, L. E. Neurons in monkey parietal area LIP are tuned for eye-movement parameters in three-dimensional space. *J. Neurophysiol.* 73: 280–297, 1995.
- GOGEL, W. C. The sensing of retinal size. *Vision Res.* 9: 1079–1094, 1969.
- GOGEL, W. C. Scalar perceptions with binocular cues of distance. *Am. J. Psychol.* 85: 477–497, 1972.
- GORDON, J., GHILARDI, M. F., AND GHEZ, C. In reaching, the task is to move the hand to a target (commentary to Flanders, M. et al.). *Behav. Brain Sci.* 15: 337–339, 1992.
- GORDON, J., GHILARDI, M. F., AND GHEZ, C. Accuracy of planar reaching movements. I. Independence of direction and extent variability. *Exp. Brain Res.* 99: 97–111, 1994.
- JIANG, B. C. Accommodative vergence is driven by the phasic component of the accommodative controller. *Vision Res.* 36: 97–102, 1996.
- KINCHLA, R. A. AND SMYZER, F. A. A diffusion model of perception memory. *Percept. Psychophys.* 15: 353–360, 1967.
- LACQUANITI, F. Frames of reference in sensorimotor coordination. In: *Handbook of Neuropsychology*, edited by F. Boller and J. Grafman. Amsterdam: Elsevier, 1997, vol. 11, p. 27–63.
- LACQUANITI, F., LE TAILLANTER, M., LOPIANO, L., AND MAIOLI, C. The control of limb geometry in cat posture. *J. Physiol. (Lond.)* 426: 1772–1792, 1990.
- MATIN, L., MATIN, E., AND PEARCE, D. G. Visual perception of direction in the dark: role of local sign, eye movements and ocular proprioception. *Vision Res.* 6: 453–469, 1966.
- MATIN, L., MATIN, E., AND PEARCE, D. G. Eye movements in the dark during the attempt to maintain prior fixation position. *Vision Res.* 10: 837–857, 1970.
- MAYS, L. E. AND GAMLIN, P.D.R. Neuronal circuitry controlling the near response. *Curr. Opin. Neurobiol.* 5: 763–768, 1995.
- MORRISON, D. F. *Multivariate Statistical Methods*. Singapore: McGraw-Hill, 1990.
- OWENS, D. A. AND LEIBOWITZ, H. W. Accommodation convergence and distance perception in low illumination. *Am. J. Optom. Physiol. Opt.* 65: 118–126, 1980.
- POULTON, E. C. Human manual control. In: *Handbook of Physiology. The Nervous System. Motor Control*. Bethesda, MD: Am. Physiol. Soc., 1981, sect. 1, vol. II, p. 1337–1389.
- PRABLANC, C., ECHALLIER, J. F., KOMILIS, E., AND JEANNEROD, M. Optimal response of eye and hand motor systems in pointing at a visual target. I. Spatio-temporal characteristics of eye and hand movements and their relationship when varying the amount of visual information. *Biol. Cybern.* 35: 113–124, 1979.
- PRESS, W. H., FLANNERY, B. P., TEUKOLSKY, S. A., AND VETTERLING, W. T. *Numerical Recipes In C*. Cambridge, UK: Cambridge Univ. Press, 1988, p. 374.
- REGAN, D., ERKELENS, C. J., AND COLLEWIJN, H. Necessary conditions for the perception of motion in depth. *Invest. Ophthalmol. Visual Sci.* 27: 584–597, 1986.
- SCHOR, C. M. A dynamic model of cross-coupling between accommodation and convergence: simulation of step and frequency responses. *Optom. Vision Sci.* 69: 258–269, 1992.
- SOECHTING, J. F. AND FLANDERS, M. Sensorimotor representations for pointing to targets in three-dimensional space. *J. Neurophysiol.* 62: 582–594, 1989a.
- SOECHTING, J. F. AND FLANDERS, M. Errors in pointing are due to approximations in sensorimotor transformations. *J. Neurophysiol.* 62: 595–608, 1989b.
- SOECHTING, J. F., TILLERY, S.I.H., AND FLANDERS, M. Transformation from head- to shoulder- centered representation of target direction in arm movements. *J. Cognit. Neurosci.* 2: 32–43, 1990.
- STEINMAN, R. M., LEVINSON, J. Z., COLLEWIJN, H., AND VAN DER STEEN, J. Vision in the presence of known natural retinal image motion. *J. Opt. Soc. Am. A* 2: 226–233, 1985.
- VAN EE, R. AND ERKELENS, C. J. Stability of binocular depth perception with moving head and eyes. *Vision Res.* 36: 3827–3842, 1996.
- WESTHEIMER, G. Cooperative neural processes involved in stereoscopic acuity. *Exp. Brain Res.* 36: 585–597, 1979.
- WHITE, J. M., SPARKS, D. L., AND STANFORD, T. R. Saccades to remembered target locations: an analysis of systematic and variable errors. *Vision Res.* 34: 79–92, 1993.